Frontiers in Integrated Science and Technological Innovation

Dr. K. ARUMUGANAINAR
Mrs. DIMPLE JUNEJA
Dr. M. KARTHICK
Dr. S. VISHNU

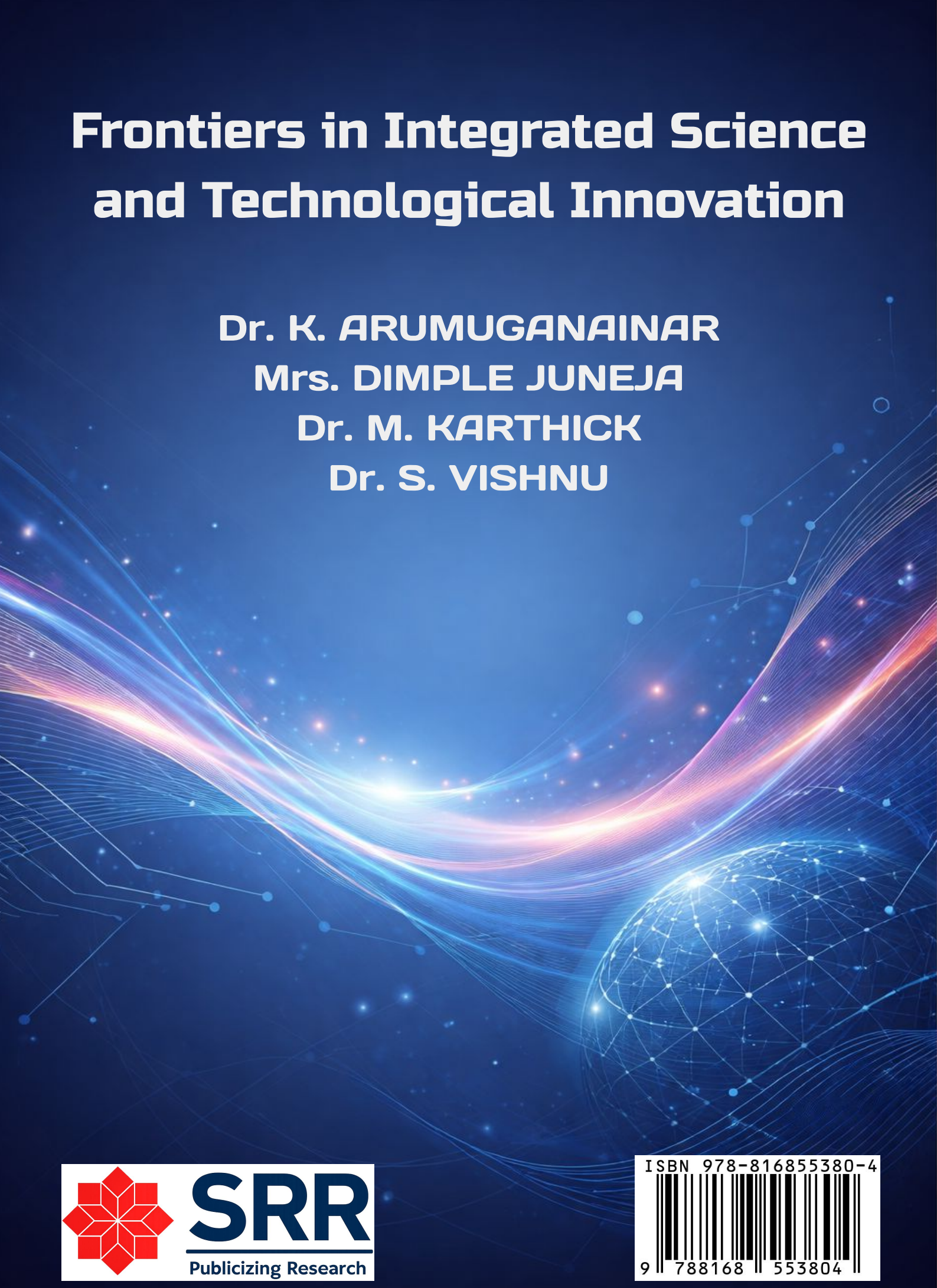

SRR
Publicizing Research

ISBN 978-816855380-4

Frontiers in Integrated Science and Technological Innovation

April 2026

Dr. K. ARUMUGANAINAR
Assistant Professor, Department of Mechanical Engineering
J.P. College of Engineering
Tenkasi, Tamil Nadu, India.

Mrs. DIMPLE JUNEJA
Research Scholar, Department of Education
Mohanlal Sukhadia University
Udaipur, Rajasthan, India.

Dr. M. KARTHICK
Assistant Professor
Department of Mechanical Engineering
Vel Tech Rangarajan Dr. Sagunthala R&D Institute of Science and Technology, Chennai, Tamil Nadu, India.

Dr. S. VISHNU
Assistant Professor, Centre for Sustainable Materials Research
Department of Mechanical Engineering
Academy of Maritime Education and Training (AMET)
Deemed to be University, Kandahar, Chennai, India.

April 2026

ISBN: 978-81-685538-0-4

ISBN 978-816855380-4

9 788168 553804

Published By

SRR
Publicizing Research

SCIENTIFIC RESEARCH REPORTS
(A Book Publisher, approved by Govt. of India)

I Floor, S S Nagar, Chennai - 600 087,
Tamil Nadu, India.

editors@srrbooks.in, contact@srrbooks.in
www.srrbooks.in

PREFACE

The rapid convergence of scientific disciplines and technological domains has redefined the landscape of modern research and innovation. ***Frontiers in Integrated Science and Technological Innovation*** is conceived as a comprehensive volume that captures this multidisciplinary evolution, bringing together diverse yet interconnected studies spanning materials science, mechanical engineering, energy systems, healthcare, social sciences, and environmental sustainability.

This book opens with an exploration of advanced materials, highlighting recent developments in polyester composites with a focus on their mechanical and tribological behavior. Such studies underline the growing importance of engineered materials in enhancing durability and performance across industrial applications. Complementing this, investigations into perovskite nanoparticles and D-Phenylglycinium derivatives provide deep insights into structural, morphological, optical, and nonlinear optical properties, emphasizing their potential in next-generation optoelectronic devices.

The volume also bridges technology with societal dimensions. The analysis of multi-generational workforce dynamics in Chennai city offers a timely perspective on organizational behavior, workplace diversity, and the challenges faced by young professionals in a rapidly evolving economic environment. This inclusion reinforces the idea that technological progress must be understood alongside human and social factors.

Healthcare advancements form another critical pillar of this collection. The discussion on recent strategies for managing Chronic Obstructive Pulmonary Disease (COPD) reflects the integration of medical research with technological interventions, aiming to improve patient outcomes and quality of life. Such contributions demonstrate the vital role of interdisciplinary approaches in addressing complex health challenges.

Engineering innovation is further showcased through studies on surface engineering and coating technologies for tool steels, as well as automotive safety systems like rear collision warning mechanisms. The structural integrity analysis of electric vehicle battery enclosures under impact conditions underscores the urgency of developing safe and reliable solutions in the transition toward sustainable mobility.

Energy and environmental sustainability are central themes woven throughout the book. Reviews on vegetable oil-based fuels and biofuels highlight alternative energy pathways for reducing emissions in compression ignition engines. These discussions are complemented by a broader examination of sustainability and environmental chemistry, focusing on principles, processes, and remediation strategies essential for addressing global ecological concerns.

Collectively, the chapters in this volume reflect a unifying vision: that innovation thrives at the intersection of disciplines. By integrating theoretical insights, experimental research, and applied technologies, this book aims to serve as a valuable resource for researchers, academicians, and industry professionals seeking to

navigate and contribute to the evolving frontiers of science and technology.

It is our hope that this compilation not only informs but also inspires further interdisciplinary collaboration and transformative innovation. We extend our sincere thanks to our publisher, Scientific Research Reports, Chennai, India, for their dedicated efforts in preparing this book and for ensuring the inclusion of enriched and high-quality technical content.

Wishes and Regards,

Dr. K. ARUMUGANAINAR
Assistant Professor, Department of Mechanical Engineering
J.P. College of Engineering
Tenkasi, Tamil Nadu, India.

Mrs. DIMPLE JUNEJA
Research Scholar, Department of Education
Mohanlal Sukhadia University
Udaipur, Rajasthan, India.

Dr. M. KARTHICK
Assistant Professor
Department of Mechanical Engineering
Vel Tech Rangarajan Dr. Sagunthala R&D Institute of Science and Technology, Chennai, Tamil Nadu, India.

Dr. S. VISHNU
Assistant Professor, Centre for Sustainable Materials Research
Department of Mechanical Engineering
Academy of Maritime Education and Training (AMET)
Deemed to be University, Kanathur, Chennai, India.

CONTENTS


SRR
Publicizing Research

Chapter 1

Recent Developments of Mechanical and Tribological Properties of Polyester Composites: A Review

T.Elaiyaraja[1], G.Manikandan[2], S.Manikandan[2], S.Susuindhar[2], S.Mukelan[2]

[1]*Assistant Professor, Department of Mechanical Engineering, Roever Engineering College, Perambalur, Tamil Nadu, India.*

[2]*UG Student, Department of Mechanical Engineering, Roever Engineering College, Perambalur, Tamil Nadu, India.*

Corresponding Author: elaiyabala18@gmail.com

Abstract

Polyester matrix composites have attracted a lot of popularity in research due to their ability to be reinforced with various materials, lightweight, and cheap processing. This review paper thoroughly discusses the experimental advancements of the last period that have been made in the mechanical and tribological properties of polyester composites reinforced with natural fibers, synthetic fibers, and hybrid particulate fillers. Properties obtained from tensile flexural hardness, and impact tests are considered along with wear rate, friction coefficient, and sliding behavior under different load and speed conditions. Failure mechanisms have been explained through microstructural correlations using SEM fractography. This review first gathers the numerical results reported in the recent literature, then points out the factors limiting the performance and finally highlights the future research areas to design high-performance, sustainable polyester composite systems.

ISBN 978-816855380-4

Keywords: Polyester matrix composites, mechanical properties, tribological behaviour, natural fibre reinforcement, wear resistance.

1. Mechanical Properties of Polyester Composites

1.1 Tensile, Flexural, and Impact Behaviour

Polyester composites reinforced with natural and synthetic fibres show a significant increase in mechanical properties that are mainly dependent on fibre volume fraction, fibre orientation, matrix fibre interfacial adhesion, and surface treatment efficiency. Glass fibre reinforced polyester (GFRP) at 40 vol.% fibre loading can deliver UTS values of 210-260 MPa and flexural strength of 280-320 MPa, which are significantly higher than unreinforced polyester (UTS 45-55 MPa) [1]. Natural fibre reinforcements jute sisal coir, and kenaf provide advantages in density (1.21.5 g/cm^3 against g/cm^3 for glass) with close specific strengths, especially after alkaline (NaOH, 510 wt.%) or silane surface treatment, which enhance fibrematrix bonding by decreasing contact angle from ~65 to ~28 and raising interfacial shear strength by 25-40%. Hybrid polyester composites made of glass and natural fibres show a positive hybridisation effect, where tensile modulus increases synergistically beyond the rule-of-mixtures prediction. Kenaf/glass hybrid polyester at 30/10 wt. % loading achieved UTS of 187 MPa and flexural modulus of 14.3 GPa, whereas kenaf/polyester gave 134 MPa and 9.8 GPa, a 39.5% and 46% increase respectively [3]. Impact strength is also in alignment with this pattern, hybrids being able to absorb 35-55 J/m while mono-reinforced natural fibre composites absorb 18-24 J/m only, which is due to mechanisms of crack deflection and fibre pull-out energy dissipation. Particulate fillers SiC, Al_2O_3, fly ash, and TiO_2 at 5-15 wt.% level improve hardness (Shore D: 78-91) and compressive

strength (85-130 MPa) while they slightly decrease elongation at break from 2.8% to 1.41.9%, this is indicative of increased stiffness and lower matrix plasticity [4].

1.2 Hardness and Microstructural Observations

Microhardness tests (Vickers, 0.5 kgf load) show that adding filler leads to stiffening. Polyester filled with 10 wt.% TiO_2 goes up to 38 HV versus 22 HV for polyester only a 72.7% raise that is due to both the great hardness of TiO_2 (900 HV) and the pinning effect of the grain boundaries of TiO_2 on the polymer network [4]. SEM fractography of tensile-failed specimens reveals three major failure modes: (i) pure matrix failure in systems without fibres or with very low fibre content, (ii) fibrematrix debonding at untreated interfaces, and (iii) mixed-mode failure with fibre fracture in alkaline-treated hybrid systems. Voids, the content of which was determined by Archimedes density measurements, were very low, varying from 1.8 to 4.5% in composites made by hand lay-up and below 1.2% in compression-moulded systems, resulting in a 15 to 22% loss in flexural strength for every 1% void rise [1].

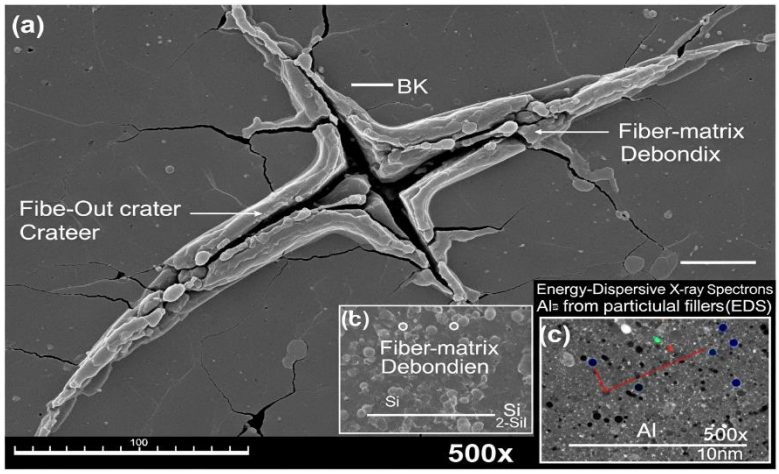

Figure 1: SEM fractograph of a hybrid polyester composite reinforced with glass and jute fibres

ISBN 978-816855380-4

2. Tribological Properties of Polyester Composites

2.1 Wear and Friction Behaviour

Table: 1: Tribological Properties of Selected Polyester Composites from Literature

Matrix	Reinforcement	Load (N)	Sliding Speed (m/s)	Wear Rate ($\times 10^{-4}$ mm^3/Nm)	Friction Coefficient (μ)	Reference
Polyester	30% Glass Fibre	20	1.0	3.12	0.38	[1]
Polyester	20% Jute + 10% Glass	30	1.5	4.85	0.44	[3]
Polyester	10% SiC + 20% Glass	25	1.0	2.34	0.32	[5]
Polyester	10% TiO_2 particulate	20	0.5	5.67	0.51	[4]
Polyester	15% Al_2O_3 + 15% Sisal	40	2.0	3.89	0.41	[6]

Dry sliding wear behavior of polyester composites, as determined by pin-on-disc tribometers according to ASTM G99, varies significantly with work load (10 to 50 N), sliding speed (0.5 to 3.0 m/s) and type of reinforcement. Specific wear rate of polyester significantly drops (by 3562%) when it is reinforced with glass fibres. This is because fibres not only carry the compressive contact stresses but also limit the polymer matrix direct contact with the counter face [1]. Use of SiC particulate (10 wt.%) reduces the wear rate even further to 2.34 10 mm/Nm by being a load-bearing third body and also by forming a protective tribofilm at the contact interface [5]. Friction coefficient falls within 0.280.55 for composite systems whereas self-lubricating graphite additions (3 to 5 wt. %) are capable of cutting down to 0.18 to 0.24 levels owing to solid lubricant film formation [6].

2.2 Erosive Wear and Elevated Temperature Tribology

Erosive wear resistance, determined at various impingement angles of 30°-90° with silica sand erodent (150-250 m, 40-60 m/s velocity), shows that polyester composites are semi-ductile materials and they experience the greatest erosion at 45-60° impingement angles. Glass/polyester composites give out an erosion rate of 8.2 mg/kg at 45 against 14.6 mg/kg for neat polyester - a 43.8% lowering that is achieved through a fibre-reinforced surface layer resistant to lateral cutting by erodent particles [7]. Exposure to high temperatures (60-100°C) causing matrix softening is equivalent to lowering hardness by 18-30% and increasing wear rate by 2.1-3.4 times which exposes the thermal stability as a major drawback. Addition of nanosilica (SiO_2, 20-50 nm) at 3 wt.% level is capable of raising wear resistance at elevated temperatures by 28% due to increased matrix crosslinking and better thermal conductivity [8].

2.3 Fabrication Methods and Their Influence on Tribological Performance

Hand lay-up, still the most popular open-mould technique, yields composites with void fractions of 2.5-4.8%, which serve as stress concentration sites during sliding contact thereby making subsurface crack nucleation faster and also the wear rate goes up by 18-25% compared to closed-mould processed counterparts [9]. Compression moulding at pressures of 5-15 MPa not only lowers void content to less than 1.2% but also enhances the fibrematrix contact area, resulting in wear rates that are 20-30% less than hand lay-up fabricated equivalents under the same tribological test conditions [6]. At controlled injection pressures (0.3-0.8 MPa), resin transfer moulding (RTM) provides excellent fibre wetting and impregnation

ISBN 978-816855380-4

uniformity producing composites with fibre volume fractions of 45-55% and void content less than 0.9%. Glass/polyester composites processed by RTM showed specific wear rates of 1.98 10 mm/Nm at 30 N load - about 36% lower than hand lay-up processed equivalents due to better interfacial bonding and fewer stress-raising voids at the tribocontact zone [5]. Vacuum-assisted resin infusion (VARI) goes a step further in removing trapped air and results in hybrid natural/synthetic fibre polyester systems with porosity close to zero (0.5%), and the coefficient of friction decreases by 12-18% as compared to the conventional casting, which is due to the surface being smoother (Ra: 0.8-1.4 μm vs. 2.1-3.6 μm in hand lay-up) and hence the adhesive wear contribution is limited [10].

Post-cure temperature is one of the most important factors affecting the tribological performance of materials. Composites post-cured at 80°C for 4 hours can have a crosslink density-level improvement in the range of 15-22% when compared with those cured at room temperature, leading to less matrix deformability under frictional heating and up to 24% reduction in steady-state wear rates at high sliding speeds (2.0-3.0 m/s) [9].

3. Conclusion

Polyester composites reinforced with hybrid fibreparticulate systems demonstrate substantial mechanical and tribological performance improvements over unreinforced matrices. Besides 39-78% tensile strength increases, hardness up to 72%, and wear rate reductions in the range of 35-62% can be achieved through optimised reinforcement selection, fibre treatment preparation and control of the production process. Alkaline and silane fibre treatments are crucial in improving the interfacial bonding, which through stress

transfer reduction of void content, besides increasing the stress transfer efficiency. From a tribological viewpoint, the use of SiC and Al_2O_3 particulates results in better wear resistance whereas the addition of graphite leads to a significant decrease in friction coefficients. Advancements in polyester composites that are capable of meeting the requirements of structural and automotive applications depend on future works that combine nano-filler hybridisation, bio-derived matrix systems, and high-temperature tribological characterisation.

References

[1] Rajesh, J. J., Bijwe, J., Tewari, U. S., & Venkataraman, B. (2001). Erosive wear behaviour of various polyamides. *Wear, 249*(8), 702–714. https://doi.org/10.1016/S0043-1648(01)00695-0

[2] Rong, M. Z., Zhang, M. Q., Liu, Y., Yang, G. C., & Zeng, H. M. (2001). The effect of fiber treatment on the mechanical properties of unidirectional sisal-reinforced epoxy composites. *Composites Science and Technology, 61*(10), 1437–1447. https://doi.org/10.1016/S0266-3538(01)00046-X

[3] Jawaid, M., & Abdul Khalil, H. P. S. (2011). Cellulosic/synthetic fibre reinforced polymer hybrid composites: A review. *Carbohydrate Polymers, 86*(1), 1–18. https://doi.org/10.1016/j.carbpol.2011.04.043

[4] Chauhan, S. R., & Thakur, S. (2013). Effects of particle size, particle loading and sliding distance on the friction and wear properties of cenosphere particulate filled vinylester composites. *Materials & Design, 51*, 398–408. https://doi.org/10.1016/j.matdes.2013.03.071

[5] Chand, N., & Fahim, M. (2008). *Introduction to Tribology of Polymers* (2nd ed.). Woodhead Publishing.

[6] Shalwan, A., & Yousif, B. F. (2013). In state of art: Mechanical and tribological behaviour of polymeric composites based on natural fibres. *Materials & Design, 48*, 14–24. https://doi.org/10.1016/j.matdes.2012.07.014

ISBN 978-816855380-4

[7] Patnaik, A., Satapathy, A., Mahapatra, S. S., & Dash, R. R. (2008). Tribo-performance of polyester hybrid composites: Damage assessment and parameter optimization using Taguchi design. *Materials & Design, 30*(1), 57–67. https://doi.org/10.1016/j.matdes.2008.04.057

[8] Wetzel, B., Haupert, F., & Zhang, M. Q. (2003). Epoxy nanocomposites with high mechanical and tribological performance. *Composites Science and Technology, 63*(14), 2055–2067. https://doi.org/10.1016/S0266-3538(03)00115-5

[9] Friedrich, K., Zhang, Z., & Schlarb, A. K. (2005). Effects of various fillers on the sliding wear of polymer composites. *Composites Science and Technology, 65*(15–16), 2329–2343. https://doi.org/10.1016/j.compscitech.2005.05.028

Chapter 2

Structural, Morphological and Surface Investigation of Perovsikte (LSNO) Nanoparticles

Jeya Priya CV[1], M Parthasarathy[1], V Gowthami[1*]

[1]*Department of Physics, School of Basic Sciences, Vels Institute of Science, Technology & Advanced Studies (VISTAS), Chennai, 600117*

** Corresponding Author: gowthamivijayakumar@gmail.com*

Abstract

Perovsikte-type transition metal oxides have emerged as promising electrode materials for next-generation energy storage systems due to their remarkable electronic conductivity, structural stability, and tunable redox properties. In the present study, lanthanum strontium nickel oxide ($LaSrNiO_3$, LSNO) nanoparticles were synthesized and systematically characterized to investigate their structural, morphological, and surface properties relevant to electrochemical applications. The crystalline phase and structural purity of the synthesized LSNO nanoparticles were confirmed using X-ray diffraction (XRD), revealing a well-defined perovskite crystal structure with sharp diffraction peaks. Fourier transform infrared spectroscopy (FTIR) analysis verified the formation of metal–oxygen bonds and confirmed the presence of characteristic vibrational modes associated with the perovskite lattice. The surface area and pore distribution were examined through Brunauer–Emmett–Teller (BET) analysis, indicating a mesoporous structure that is favorable for electrolyte ion diffusion and enhanced electrochemical activity. Morphological examination using scanning electron microscopy (SEM) revealed agglomerated nanoscale particles with irregular yet porous surface

ISBN 978-816855380-4

textures, which provide abundant active sites for charge storage processes. Elemental composition and chemical purity were validated by energy-dispersive X-ray spectroscopy (EDAX), confirming the presence of La, Sr, Ni, and O elements without significant impurities. The combined structural and surface analyses suggest that LSNO nanoparticles possess desirable physicochemical properties suitable for high-performance electrochemical energy storage devices such as super capacitors. These findings provide valuable insights into the design and optimization of Perovsikte-based electrode materials for advanced energy storage technologies.

Keywords: Perovsikte oxide, Nano material, Transition metal Oxide, LSNO nanoparticles, BET surface area, Energy storage devices.

Graphical Abstract

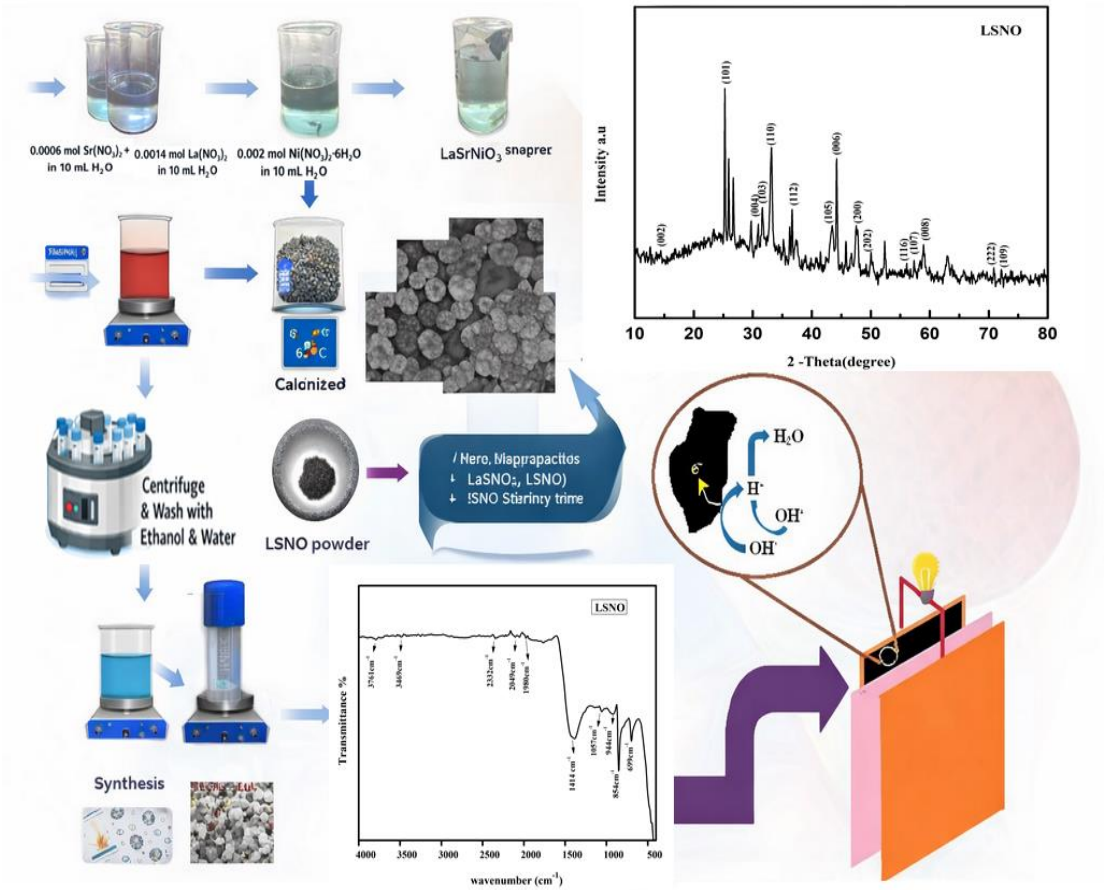

1. Introduction

The rapid growth of global energy demand and the increasing reliance on renewable energy sources have driven significant research interest toward the development of efficient and sustainable energy storage technologies. Among the various energy storage systems, electrochemical supercapacitors have gained considerable attention due to their high power density, fast charge–discharge capability, and long cycling stability compared with conventional batteries[1] However, the performance of supercapacitors largely depends on the properties of electrode materials, particularly their electrical conductivity, surface area, and redox activity. Therefore, the development of advanced electrode materials with improved electrochemical characteristics has become a critical research focus in recent years.

Transition metal oxides have emerged as promising candidates for energy storage applications owing to their multiple oxidation states, good electrochemical activity, and structural versatility. In particular, perovskite-type oxides with the general formula ABO_3 have attracted significant interest due to their flexible crystal structure and tunable physicochemical properties. In this structure, the A-site is typically occupied by rare-earth or alkaline-earth metals, while the B-site is occupied by transition metals. The interaction between these cations leads to unique electrical, magnetic, and catalytic properties, making perovskite oxides suitable for applications in catalysis, fuel cells, sensors, and electrochemical energy storage systems. Lanthanum-based perovskite oxides have been widely investigated because of their excellent electronic conductivity and structural stability. Among them, lanthanum strontium nickel oxide ($LaSrNiO_3$, LSNO) has gained increasing attention as an efficient electrode material due to

ISBN 978-816855380-4

its enhanced electrical conductivity and favorable redox characteristics arising from the mixed valence states of nickel ions [2]. The substitution of lanthanum with strontium at the A-site introduces oxygen vacancies and improves charge transport properties, which significantly enhances the electrochemical activity of the material. These characteristics make LSNO a promising candidate for high-performance supercapacitor electrodes. In addition to composition, the electrochemical performance of perovskite materials is strongly influenced by their morphology, particle size, and surface area. Nanostructured materials typically exhibit improved electrochemical performance due to their large surface-to-volume ratio and shorter ion diffusion pathways.

Therefore, controlling the synthesis process to obtain nanoscale perovskite particles with desirable surface characteristics is essential for optimizing their energy storage performance. Various synthesis techniques such as sol–gel, hydrothermal, combustion, and co-precipitation methods have been employed to prepare perovskite oxide nanoparticles [3]. Among these methods, the sol–gel approach offers several advantages, including better compositional control, homogeneous mixing of precursor ions, and the ability to produce highly crystalline nanostructures at relatively lower temperatures. Furthermore, the method allows precise tuning of particle size and morphology, which is critical for improving electrochemical performance. In order to evaluate the suitability of LSNO nanoparticles for energy storage applications, comprehensive characterization of their structural, morphological, and surface properties is required. X-ray diffraction (XRD) analysis provides essential information regarding the crystalline phase and structural integrity of the synthesized material. Fourier transform infrared

spectroscopy (FTIR) helps identify functional groups and metal–oxygen bonding interactions within the lattice. Surface area and porosity measurements using Brunauer–Emmett–Teller (BET) analysis are crucial for understanding ion accessibility and electrolyte interaction during electrochemical processes. Additionally, scanning electron microscopy (SEM) enables the observation of particle morphology and aggregation behavior, while energy dispersive X-ray analysis (EDAX) confirms elemental composition and purity. In this work, LSNO nanoparticles were synthesized and systematically characterized using XRD, FTIR, BET, SEM, and EDAX techniques[4] The aim of this study is to investigate the structural and surface characteristics of LSNO nanoparticles and evaluate their potential as electrode materials for electrochemical energy storage applications. The obtained results provide valuable insights into the relationship between material structure and performance, contributing to the development of advanced perovskite-based energy storage systems.

2. Synthesis of LSNO Nanomaterial

Lanthanum strontium nickel oxide (LSNO) nanoparticles with the general perovskite formula ABO_3 were synthesized by separately dissolving the A-site precursors (La and Sr salts) and the B-site precursor (Ni salt). As illustrated in Fig. 1, 0.002 mol of $Ni(NO_3)_2{\cdot}6H_2O$ was dissolved in 10 mL of distilled water and magnetically stirred for 15 minutes to obtain a clear solution. In a separate beaker, 0.0006 mol of $Sr(NO_3)_2$ and 0.0014 mol of $La(NO_3)_3{\cdot}6H_2O$ were dissolved in 10 mL of distilled water and stirred for 15 minutes to ensure complete dissolution. Subsequently, the two precursor solutions were combined and continuously stirred for an additional 30 minutes to obtain a homogeneous mixture of Ni^{2+}, La^{3+}, and Sr^{2+} ions. The resulting mixed solution was then slowly introduced into 10 mL of 1

ISBN 978-816855380-4

M NaOH solution under constant stirring conditions. Upon the addition of NaOH, the solution immediately changed to a light brown color, and after approximately two hours of continuous stirring, a blue precipitate was observed. The obtained precipitate was collected and repeatedly centrifuged using ethanol and distilled water in order to remove residual ions and possible impurities. After the purification process, the collected material was dried in a hot air oven at 60 °C overnight. The dried product was then finely ground using a mortar and pestle to obtain a uniform powder. Finally, the powder was calcined in air at 750 °C for 3 hours, resulting in the formation of highly crystalline LSNO nanoparticles.

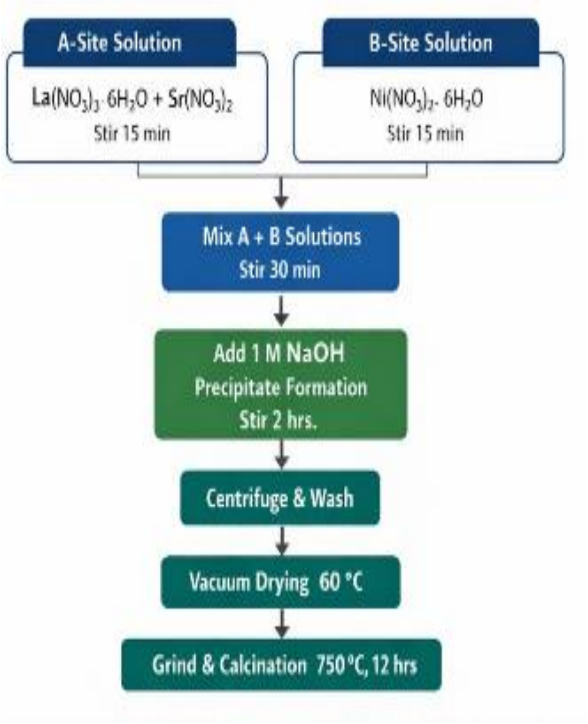

Figure 1: Synthesis of LSNO powder

3. Results and Discussion

3.1 X-ray Diffraction (XRD) Analysis

The crystal structure and phase purity of the synthesized LSNO nanoparticles were investigated using X-ray diffraction analysis. The

XRD pattern exhibits several well-defined diffraction peaks corresponding to the characteristic planes of the perovskite structure[5] Prominent peaks were observed at diffraction angles corresponding to planes such as (101), (110), (112), (105), (200), and (222), indicating the formation of a crystalline perovskite phase. The sharpness and intensity of the diffraction peaks suggest a high degree of crystallinity in the synthesized material. No significant impurity peaks were detected in the diffraction pattern, confirming the successful formation of phase-pure LSNO nanoparticles [6]. The crystalline structure of the material plays a crucial role in facilitating electron transport and improving electrochemical performance. The average crystallite size of the synthesized LSNO nanoparticles can be estimated using the Debye–Scherrer equation:

$$D=0.9\lambda/\beta\cos\theta \quad (1)$$

Where D represents the crystallite size, λ is the wavelength of the X-ray radiation, β is the full width at half maximum (FWHM) of the diffraction peak and θ is the Bragg diffraction angle.

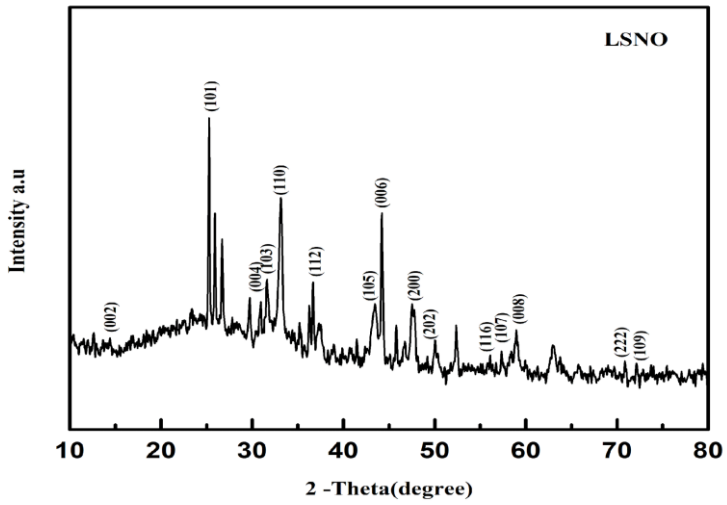

Figure 2: XRD patterns of LSNO sample

ISBN 978-816855380-4

The nanoscales crystallite size obtained from the analysis indicates that the synthesized LSNO material possesses a large active surface area suitable for electrochemical reactions.

3.2 FTIR Analysis

Fourier transform infrared spectroscopy was employed to identify the chemical bonding and functional groups present in the LSNO nanoparticles. The FTIR spectrum shows several absorption bands corresponding to different vibrational modes of the material. The broad absorption band observed around 3400–3700 cm^{-1} is attributed to the stretching vibration of hydroxyl (–OH) groups, which may arise from adsorbed moisture on the surface of the nanoparticles. Peaks located around 2300–2000 cm^{-1} correspond to the presence of atmospheric CO_2 adsorption. A strong absorption band appearing near 600–700 cm^{-1} is assigned to the metal–oxygen stretching vibration associated with the Ni–O bond in the perovskite lattice.

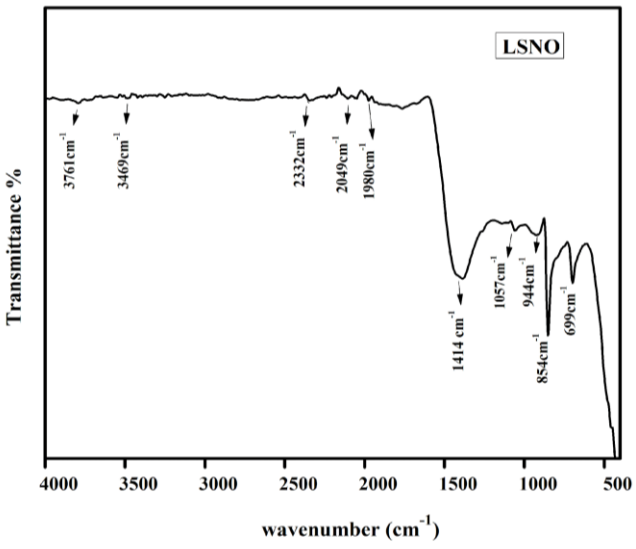

Figure 3: FT-IR spectra of LSNO

This band confirms the formation of the LSNO perovskite framework. Additional peaks observed around 850–1000 cm^{-1} are attributed to lattice vibrations and metal–oxygen bending modes within the oxide structure. These FTIR results confirm the successful formation of the metal–oxygen network characteristic of perovskite oxide materials.

3.3 BET Surface Area Analysis

The surface area and porosity of the LSNO nanoparticles were analyzed using nitrogen adsorption–desorption measurements based on the BET method. The obtained isotherm exhibits a typical adsorption–desorption behavior indicating the presence of mesoporous structures within the material. The gradual increase in nitrogen adsorption with increasing relative pressure suggests the presence of interconnected pores and a relatively high surface area [7].

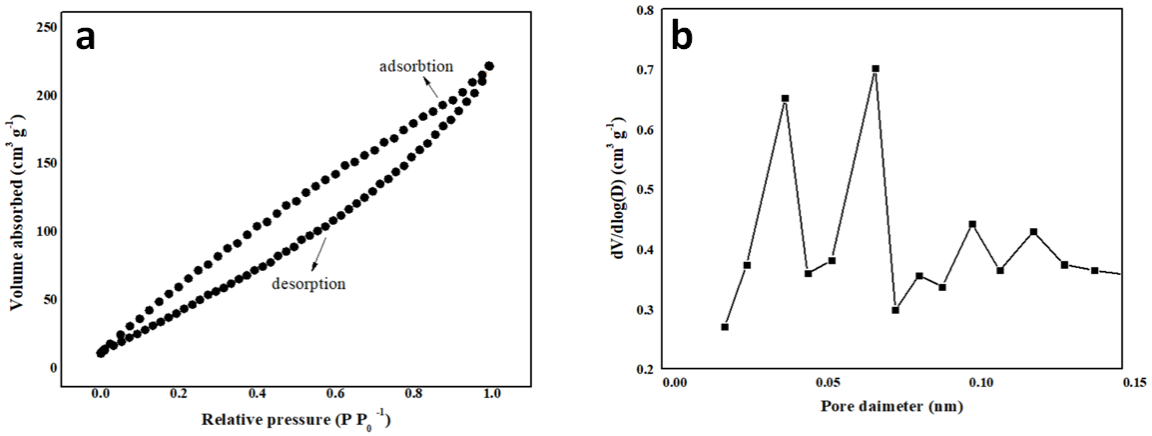

Figure 4: (a) N2 adsorption-desorption isotherms and (b) Pore Size distribution of the LSNO sample

The mesoporous nature of the material facilitates efficient ion diffusion and electrolyte penetration, which are essential for improved electrochemical performance in supercapacitor applications. The pore size distribution curve indicates the presence of pores in the

ISBN 978-816855380-4

nanometer range, further confirming the mesoporous structure of the LSNO nanoparticles.

3.4 SEM Analysis

The surface morphology of the synthesized LSNO nanoparticles was examined using scanning electron microscopy. The SEM images reveal that the particles possess a clustered and agglomerated morphology with irregular shapes. The individual particles appear to be in the nanoscale range and form interconnected networks. Such agglomerated nanostructures provide a porous architecture that can enhance electrolyte accessibility and increase the number of electrochemically active sites. The rough surface texture observed in the SEM images further contributes to improved charge storage behavior by facilitating rapid ion transport [8].

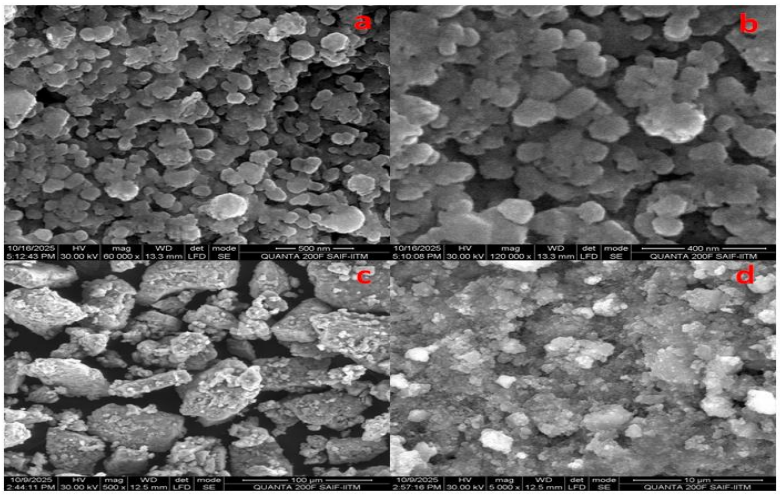

Figure 5: SEM image of LSNO, (a-d) for as prepared

3.5 EDAX Analysis

Energy dispersive X-ray spectroscopy was performed to determine the elemental composition of the synthesized LSNO nanoparticles. The EDAX spectrum clearly shows the presence of lanthanum (La), strontium (Sr), nickel (Ni), and oxygen (O) elements, confirming the

successful formation of the intended perovskite compound. The quantitative elemental analysis reveals weight percentages of approximately La (24.99%), Ni (25.98%), Sr (30.96%), and O (18.06%), which are consistent with the stoichiometric composition of LSNO. The absence of additional impurity peaks indicates the high purity of the synthesized material.

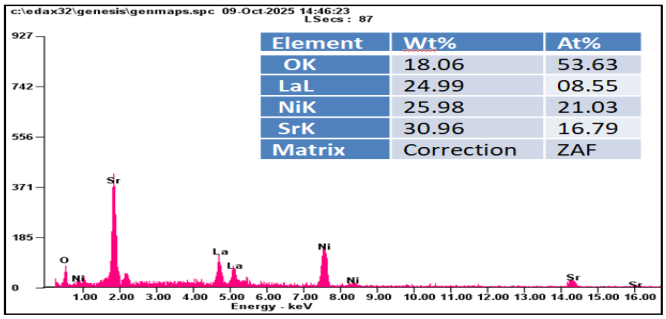

Figure 6: EDAX for LSNO sample.

4. Conclusion

In summary, lanthanum strontium nickel oxide (LSNO) nanoparticles were successfully synthesized and systematically characterized to evaluate their structural and surface properties for energy storage applications. XRD analysis confirmed the formation of a highly crystalline perovskite phase without detectable impurities. FTIR spectroscopy verified the presence of characteristic metal–oxygen bonds associated with the LSNO lattice structure. BET analysis revealed a mesoporous architecture with a relatively high surface area, which is beneficial for electrolyte diffusion and electrochemical activity. SEM observations demonstrated nanoscale particles with agglomerated and porous morphology, providing abundant active sites for charge storage processes. EDAX analysis confirmed the elemental composition and purity of the synthesized material.Overall, the structural integrity, porous morphology, and favorable surface

ISBN 978-816855380-4

characteristics of LSNO nanoparticles indicate their strong potential as electrode materials for high-performance supercapacitor and energy storage devices. Future work will focus on evaluating the electrochemical performance of LSNO-based electrodes and exploring composite structures to further enhance their energy storage capability.

References

[1] Hou, Y., Chen, L., Zhang, L., Kang, J., Fujita, T., Jiang, J., & Chen, M. (2013). Ultrahigh capacitance of nanoporous metal enhanced conductive polymer pseudocapacitors. Journal of Power Sources, 225, 304–310.

[2] Wang, G., Zhang, L., & Zhang, J. (2012). A review of electrode materials for electrochemical supercapacitors. Chem. Soc. Rev., 41(2), 797–828. https://doi.org/10.1039/C1CS15060J

[3] Xu, X., Liang, J., Zhou, H., Ding, S., & Yu, D. (2014). The preparation of hierarchical tubular structures comprised of NiO nanosheets with enhanced supercapacitive performance. RSC Adv., 4(7), 3181–3187. https://doi.org/10.1039/C3RA45038D.

[4] Hu, Q., Yue, B., Shao, H., Yang, F., Wang, J., Wang, Y., & Liu, J. (2021). Facile syntheses of perovskite type LaMO3 (M=Fe, Co, Ni) nanofibers for high performance supercapacitor electrodes and lithium-ion battery anodes. Journal of Alloys and Compounds, 852, 157002. https://doi.org/10.1016/j.jallcom.2020.157002.

[5] Cao, Y., Lin, B., Sun, Y., Yang, H., & Zhang, X. (2015). Sr-doped Lanthanum Nickelate Nanofibers for High Energy Density Supercapacitors. Electrochimica Acta, 174, 41–50.

[6] Liu, X., Hong, R., & Tian, C. (2009). Tolerance factor and the stability discussion of ABO3-type ilmenite. Journal of Materials Science: Materials in Electronics, 20(4), 323–327. https://doi.org/10.1007/s10854-008-9728-8.

[7] Zhang, B., Liu, P., Li, Z., & Song, X. (2021). Synthesis of two-dimensional sr-doped lanio3 nanosheets with improved electrochemical performance for energy storage. Nanomaterials, 11(1), 1–13. https://doi.org/10.3390/nano11010155.

Chapter 3

Synthesis, Growth, Structural, Optical Assessments and Second Order NLO Studies of D-Phenylglycinium Derivatives for Optoelectronic Applications

M Mohanraj[1], V Gowthami[1], M Parthasarathy[1*]

[1]*Department of Physics, School of Basic Sciences, Vels Institute of Science, Technology & Advanced Studies (VISTAS), Chennai, 600117*

** Corresponding Author: mps2k7@gmail.com*

Abstract

The domain of nonlinear optics is witnessing considerable expansion, incorporating knowledge from multiple scientific areas, such as physics, chemistry, optics, crystal growth, optoelectronics, and engineering. The study of nonlinear optics garners significant attention in organic-inorganic blend compounds, owing to their diverse properties that find applications in various fields. In-depth investigations have concentrated on the non-linear optical characteristics of organic and semi-organic crystals, which hold promising applications in device fabrication. A single crystal of D-phenylglycine derivatives, including Bis(D-phenylglycinium) sulfate monohydrate (BDPGS) and D-phenylglycine hydrochloride (DPGCL), were synthesized and grown through the slow evaporation method utilizing water as a solvent. The single crystal XRD analysis demonstrated that BDPGS crystallizes in the monoclinic space group $P2_1$, while DPGCL crystallizes in the orthorhombic space group $P2_12_12$. The optical properties of the compounds were characterized through UV-Visible absorption and reflectance spectra, revealing cut-off wavelengths of 230 nm and 228 nm for BDPGS and DPGCL,

ISBN 978-816855380-4

respectively. This indicates a bandgap of 5.4 eV, suggesting superior optical quality for potential applications. The notably low Urbach energy indicates that the crystal is nearly devoid of defects, thereby maintaining its structural integrity and evaluation of refractive index demonstrated the compounds' promising optical behavior. The effectiveness of the second harmonic generation for the synthesized crystals was clearly demonstrated using the Kurtz Perry powder method, validating both the crystals shows tremendous potential for advanced technological applications.

Keywords: Slow evaporation method, X-ray diffraction, Structural, Optical bandgap, Nonlinear analysis.

1. Introduction

The prevalence of blended materials is rapidly rising, driven by their diverse and impactful applications in fields such as medicine, industry, and materials science. These innovative materials are characterized by their conjugate structures, efficiency, and remarkable chemical adaptability, which bestow exceptional electrical, magnetic, and optical properties [1]. The realm of nonlinear optics is particularly captivated by organic-inorganic blend compounds, owing to their versatility and wide-ranging applicability across various sectors [2]. Extensive research has examined organic and semi-organic crystals' non-linear optical (NLO) properties, highlighting their potential for integration in advanced device fabrication. These crystals offer advantages such as swift response times and high damage thresholds, making them indispensable in modern technology. Notably, organic crystals are exceptionally significant for NLO applications, often showcasing efficiency levels surpassing traditional potassium dihydrogen phosphate (KDP)

crystals [3]. D-Phenylglycine, an aromatic mono-amino carboxylic acid, is distinguished by the presence of a nonpolar group in its side chain, which includes a benzene ring that contributes to its remarkable properties. This compound is a promising precursor in synthesizing semi-synthetic penicillin's and cephalosporins [4]. Recent investigative studies have delved into using phenylglycine derivatives in developing cutting-edge antitumor medications and their effectiveness in mitigating inflammation. Additionally, emerging research suggests their valuable role in enhancing the delivery and absorption of L-DOPA, a crucial therapeutic agent for various medical conditions [5]. This amino acid is not only fascinating in its own right but also acts as a vital precursor in the synthesis of β-lactam antibiotics, such as semisynthetic cephalosporins and penicillin's [6]. Derivatives of D-phenylglycine, including D-phenylglycinium bromide [7], D-phenylglycinium nitrate [8], and D-phenylglycinium perchlorate [9], are currently under intense research due to their interesting physical and chemical properties. In this exciting context, we have embarked on a significant research initiative to grow high-quality non-linear optical single crystals of D-phenylglycine derivatives such as Bis(D-phenylglycinium) sulfate monohydrate (BDPGS) and D-phenylglycine hydrochloride (DPGCL). This synthesis employs a low-temperature solution growth technique, utilizing water as the solvent at ambient temperature. Therefore, our current investigation aims to elucidate key characteristics, including single-crystal X-ray diffraction, UV-Vis transmittance and reflectance studies, and studies on optical parameters such as Urbach energy, steepness parameter, refractive index and SHG studies. This process not only demonstrates the potential of D-phenylglycine derivatives

ISBN 978-816855380-4

but also supports further research and applications in advanced optical technologies.

2. Experimental Procedure

2.1 Synthesis and growth of BDPGS

The synthesizing of the sulfuric acid admixture D-Phenylglycinium was meticulously executed by first dissolving high-purity D-Phenylglycine in concentrated sulfuric acid within a carefully measured volume of distilled water. This was performed following a precise stoichiometric ratio of 2:1. The solution was gently stirred for eight hours at a stable temperature of 35°C to achieve a uniform mixture, promoting complete solubility and homogeneity. Once the solution reached the desired consistency, it was filtered through Whatman filter paper, ensuring the removal of any impurities, and transferred into a thoroughly cleaned beaker. This beaker was then covered with a polythene sheet adorned with numerous small perforations, facilitating a controlled and gradual evaporation process. After three weeks, the slow and methodical evaporation yielded an exquisite, transparent single crystal of Bis (D-Phenylglycinium) Sulphate Monohydrate (BDPGS), as shown in Figure 1a.

2.2 Synthesis and growth of DPGCL

To prepare a concentrated solution, D-phenylglycine was carefully mixed with hydrochloric acid in a precise 1:1 ratio and dissolved in distilled water at 35°C. The mixture was then stirred vigorously for six hours to ensure a uniform and homogeneous solution. After thorough mixing, the solution was filtered through Whatman filter paper to remove any impurities. It was then placed in a controlled environment free from mechanical disturbances and thermal

vibrations, allowing the process to proceed naturally. Over several days, the slow and methodical evaporation yielded an exquisite, transparent single crystal of D-phenylglycine hydrochloride, as shown in Figure 1b.

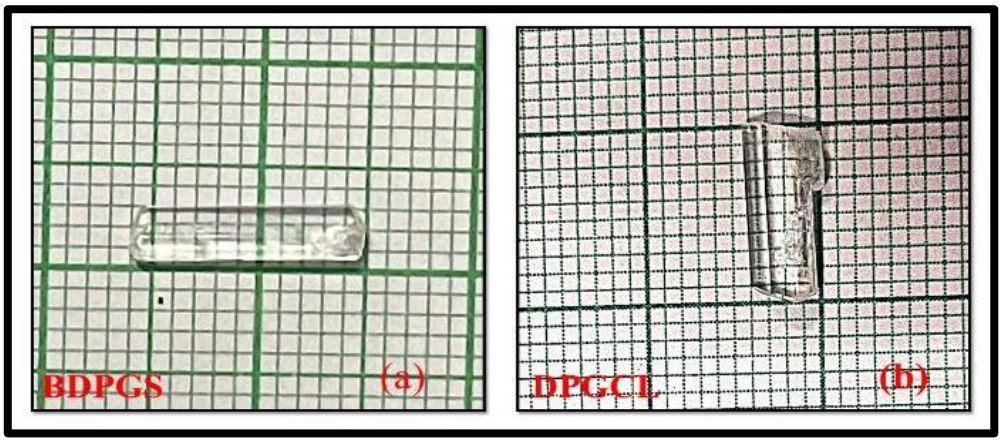

Figure. 1: As grown single crystals of (a) BDPGS (b) DPGCL

3. Results and Discussion

3.1 Single Crystal X-Ray Diffraction Analysis

Table 1. Single-crystal XRD parameters of BDPGS and DPGCL

Lattice Parameters	**Present Work (BDPGS)**	**N. Srinivasan et al. [10]**
a (Å)	12.328(3)	12.3201(12)
b (Å)	5.936(12)	5.9377(15)
c (Å)	14.296(3)	14.2908(16)
α = γ (°)	90	90
β (°)	111.335 (11)	111.369(10)
Crystal System	Monoclinic	Monoclinic
Space group	$P2_1$	$P2_1$
Lattice Parameters	**Present Work (DPGCL)**	**S. Ravichandran et al. [11]**
a (Å)	5.452(17)	5.437(5)
b (Å)	7.278(2)	7.257(8)
c (Å)	22.819(1)	22.773(2)
α = β = γ (°)	90	90
Crystal System	Orthorhombic	Orthorhombic
Space group	$P2_12_12_1$	$P2_12_12_1$

ISBN 978-816855380-4

The Brucker D8 Quest SCXRD, which utilizes Mo-Kα radiation at ambient temperature, was employed to meticulously investigate and determine the cell parameters of the synthesized crystals of BDPGS and DPGCL. The lattice parameters for this intriguing material are measured, and notably, these values correlate strongly with those previously reported in the literature [10,11], underscoring the reliability of the synthesis and characterization process, as tabulated in Table 1.

3.2 Optical Studies

3.2.1 UV-Visible Absorbance Analysis

The UV-Vis analysis offers a compelling glimpse into the complex interplay between the electronic bandgap, atomic structure, and crystalline characteristics of the material. Our extensive absorption studies on the synthesized compound spanned a broad spectrum of wavelengths, from 200 to 800 nm, providing a thorough examination of its optical properties. The results detailed in Figures 2a and 2b reveal an impressive level of reflectance throughout the visible region, marking this material as an intriguing candidate for further scientific investigation [12]. Notably, Figures 2a and 2b highlight a significant cut-off wavelength at 230 nm and 228 nm for BDPGS and DPGCL, which serves as an important threshold in defining the optical features of the material. To gain deeper insights into its properties, we apply Tauc's relation (1), which serves as an essential framework for calculating the absorption coefficient:

$$(\alpha h\nu)^n = T\,(h\nu - Eg) \qquad (1)$$

In this equation, the exponent n varies based on the type of bandgap present: n=1/2 indicates a direct bandgap, while n=2 pertains to an indirect bandgap. The resulting Tauc's plot, depicted in Figures 3a

and 3b, indicates that the materials possess an optical bandgap energy of 5.4 eV. This striking revelation underscores the material's promising potential for nonlinear optical applications. Furthermore, this finding suggests that the material boasts a remarkably low concentration of defects, thus opening pathways for innovative applications in advanced photonic devices [13].

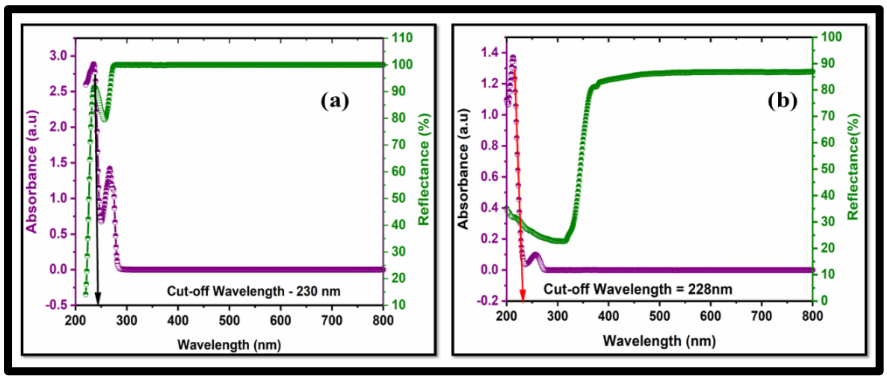

Figure 2: UV-Vis Absorbance and Reflectance spectrum of (a) BDPGS (b) DPGCL

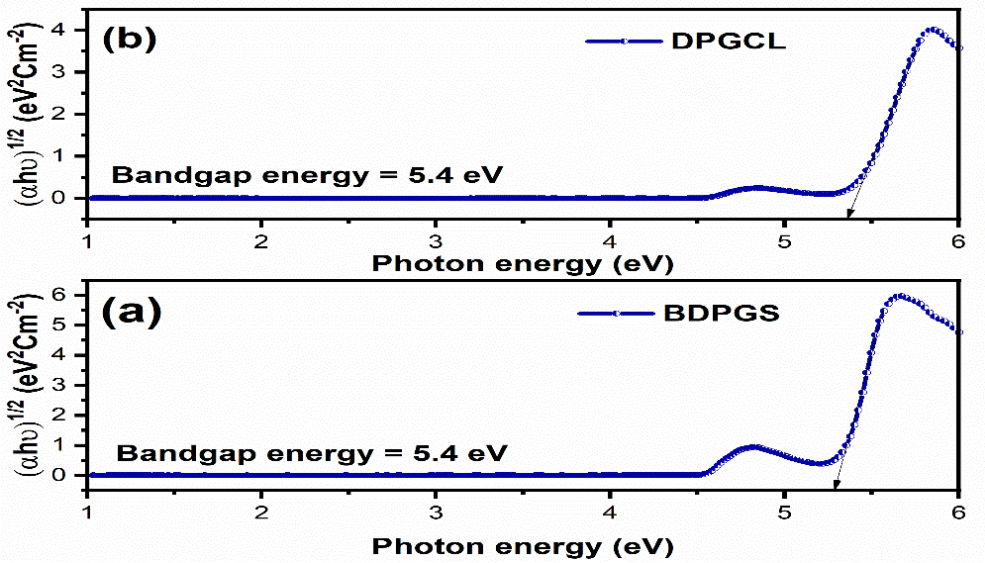

Figure 3: Bandgap Spectrum of (a) BDPGS (b) DPGCL

3.3 Absorption Band Tail

The significance of optical absorption in material science cannot be overstated, as it enables the assessment of a material's

ISBN 978-816855380-4

appropriateness for optical applications by offering vital information regarding its optical bandgap. The optical absorption spectra exhibit three distinct regions: a prominent area that denotes the optical bandgap, a subdued section that suggests the existence of flaws and impurities, and an absorption edge that illustrates variations and disruptions within the lattice structure [14]. Next to the optical bandgap on the absorption coefficient curve lies an exponential region referred to as the Urbach tail. The exponential tail, also known as Urbach energy, plays a crucial role in weakly crystalline materials and shows a notable reduction in well-crystalline specimens [15]. An exponential equation illustrates the connection between the absorption coefficient (α) and photon energy, known as the Urbach empirical rule.

$$\alpha = \alpha_o exp\left(\frac{h\nu}{E_u}\right) \qquad (2)$$

$$ln(\alpha) = ln\,(\alpha_o) + ln\frac{h\nu}{E_u} \qquad (3)$$

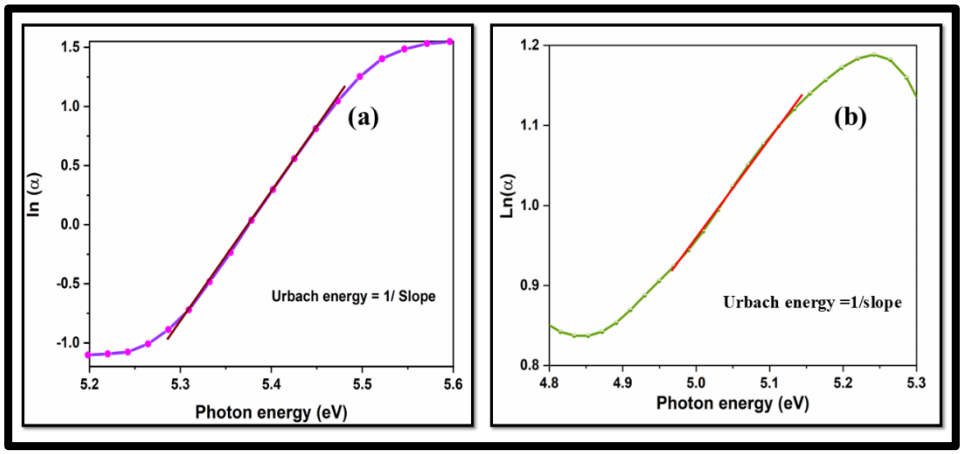

Figure 4: Plot of Photon energy (hν) vs ln (α)

In this equation, the E_U denotes the Urbach energy. The examination of the graph shown in Figures 4a and 4b, which presents photon energy against ln(α), indicates that the inverse of the slope is

associated with an Urbach energy of BDPGS and DPGCL, measured at 0.1101 eV and 0.858 eV, respectively. This observation indicates that the materials are free from imperfections and lattice disorder [16]. Additionally, Urbach identified a secondary relationship between the absorption coefficient and the optical bandgap, as detailed in equations (4-5).

$$\alpha = \beta \exp\left[\frac{\sigma(h\nu - E_o)}{K_B T}\right] \qquad (4)$$

$$\left(\frac{h\nu}{E_U}\right) = \left(\frac{\sigma(h\nu)}{K_B T}\right) \qquad (5)$$

Here, E_U is Urbach energy, K_B denotes the Boltzmann constant, and T represents the absolute temperature. The steepness parameter (σ) is determined through equation (6),

$$\sigma = \frac{K_B T}{E_U} \qquad (6)$$

Additionally, the strength of the electron-photon interaction ($E_{e\text{-}p}$) is calculated using equation (7),

$$E_{e\text{-}p} = \frac{2}{3\sigma} \qquad (7)$$

Table 2. Urbach energy and its key parameters of BDPGS and DPGCL

Description	**BDPGS**	**DPGCL**
Wavelength of absorption edge (nm)	230 nm	228 nm
Optical bandgap E_g	5.4 eV	5.4 eV
Urbach Energy E_U	0.110 eV	0.858 eV
Steepness parameter σ	0.2138	0.2742
Electron-photon interaction energy $E_{e\text{-}p}$	3.11	2.43

Table 2 summarises the values for the cut-off wavelength (nm), optical band gap energy (E_g), Urbach energy (E_U), steepness parameter (σ), and electron-photon energy ($E_{e\text{-}p}$), of BDPGS and DPGCL indicating that the materials possess exceptional

ISBN 978-816855380-4

characteristics and demonstrates significant potential for device fabrication [17].

3.4 Determination of Optical Constant

The optical constants, including optical conductivity, refractive index, and extinction coefficient, play a vital role in fabricating nonlinear optical devices. It is essential to use materials with exceptional optical quality and an excellent refractive index to develop effective devices such as optical switches and organic light-emitting diodes. The refractive index is exclusively determined by the material's composition and reflective properties [18]. According to equation (8), the refractive index can be derived from reflectance measurements.

$$n = \frac{-(R+1) \pm \sqrt{(-3R^2+10R-3)}}{2(R-1)} \qquad (8)$$

The plot presented in Figure. 5a and 5b demonstrates that the materials refractive index is measured to be 1.370 and 1371 for BDPGS and DPGCL at a wavelength of 532 nm [19].

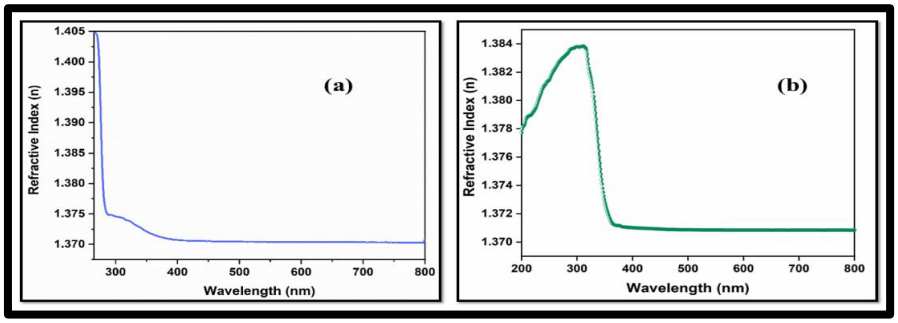

Figure 5: Wavelength (nm) vs Refractive index (n)

The reduction in the refractive index, coupled with strong transmission across the visible spectrum, indicates that the material possesses enhanced efficiency for optical applications.

3.5 Second Order Nonlinear Optical Studies

The second-harmonic generation (SHG) conversion efficiency of the sample was carefully evaluated using the Kurtz-Perry powder technique, a widely recognised method in the field [20]. For this analysis, powdered potassium dihydrogen phosphate (KDP) served as a standard reference material, given its well-established SHG properties. A high-intensity, Q-switched Nd: YAG laser emitting a fundamental wavelength of 1064 nm was used as the optical source for the experiment.

Table 3. SHG efficiency of various semi organic material with respect to KDP

Nonlinear Optical Materials	SHG efficiency
L-Glycine thiourea [22]	0.60
Diglycine hydrobromide [23]	0.80
Thiourea urea zinc sulphate [24]	0.82
Glycine Zinc Sulfate [25]	1.20
Bis(D-Phenylglycinium) sulfate monohydrate [present study]	1.23
D-phenylglycine hydrochloride [present study]	1.35

This powerful laser is known for its effectiveness in producing nonlinear optical effects. As expected, the SHG process was confirmed by the detection of green light at 532 nm, clearly indicating the material's nonlinear optical response. At an input energy of 0.7 J, the SHG output for the BDPGS compound was 6.6 mJ and DPGCL was about 7.2 mJ, significantly exceeding the KDP reference, which recorded an output of 5.4 mJ. This notable result showed that the SHG efficiency of the BDPGS was 1.23 times and DPGCL is 1.35 times greater than that of KDP, demonstrating its superior nonlinear optical performance and is compared with other NLO materials as shown in

ISBN 978-816855380-4

Table 3. Additionally, it was observed that the SHG efficiency tends to increase with larger particle size [21], suggesting that optimising particle dimensions could lead to further improvements in SHG efficiency.

4. Conclusion

A high-quality nonlinear single crystal of Bis(D-phenylglycinium) sulphate monohydrate and D-phenylglycine hydrochloride was carefully synthesized using the solution growth method of slow evaporation, with distilled water as the solvent to guarantee purity. Thorough XRD investigations revealed that the crystal BDPGS features a notable monoclinic structure, classified under the space group $P2_1$, while DPGCL exhibits an orthorhombic system with the space group $P2_12_12$, highlighting its distinctive crystalline arrangement. The optical properties of the crystals were clarified, revealing a lower cutoff wavelength of 230 nm for BDPGS and 228 nm for DPGCL, which corresponds to a notable bandgap energy of 5.4 eV. The exceptionally low Urbach energy indicates that the crystal is nearly devoid of defects, thereby maintaining its structural integrity and evaluation of refractive index demonstrated its encouraging optical characteristics. The effectiveness of the second harmonic generation for the synthesized crystal of BDPGS and DPGCL was clearly demonstrated using the Kurtz method, affirming its diverse potential for advanced technological applications.

References

[1] C.R. Kagan, D.B. Mitzi, and C.D. Dimitrakopoulos, “Organic-Inorganic Hybrid Materials as Semiconducting Channels in Thin-Film Field-Effect Transistors”, Science, vol. 286, 945, 1999, doi: 10.1126/science.286.5441.945

[2] J. Zyss, and Ed, “Molecular Nonlinear Optics: Materials, Physics and Devices”, Academic Press, Boston 1994. doi: 10.1002/adma.19950070232

[3] K. Bouchouit, Z. Sofiani, N. Benali-Cherif, L. Bendheif, A. Migalska-Zalas, and I.V. Kityk, “Third order nonlinear optical properties of hybrid mono crystals with n-conjugated systems”, 2005 7th International Conference Transparent Optical Networks, Barcelona, Spain vol.2, p.367-371, 2005, doi: 10.1109/ICTON.2005.1506175.

[4] K. Bouchouit, L. Bendheif, and N. Benali-Cherif, “D-Phenylglycinium nitrate”, Acta Cryst. E, vol.60, p.272-274, 2004, doi: 10.1107/S1600536804000972

[5] Jun Cheng, Guochao Xu, Ruizhi Han, Jinjun Dong and Ye Ni, “Efficient access to L-phenylglycine using a newly identified amino acid dehydrogenase from Bacillus clausii”, RSC Adv, vol.6, p.80557, 2016, doi: 10.1039/C6RA17683F

[6] Łukasz Wołoszyn, Maria M. Ilczyszyna, Vasyl Kinzhybalo, “The dehydration process in the DL-phenylglycinium trifluoromethanesulfonate monohydrate crystal revealed by XRD, vibrational and DSC studies”, Acta Cryst. C vol.75, p.1569-1579, 2019, doi: 10.1107/S2053229619014402

[7] M. Parthasarathy, K. Arun Kumar, R. Gopalakrishnan, “D-phenylglycinium bromide”, Acta Cryst.E vol.69, p.470, 2013, doi: 10.1107/S1600536813004807

[8] K. Bouchouit, L. Bendheif, N. Benali-Cherif, “D-phenylglycinium nitrate”, Acta Cryst. E vol.60, p.272-274, 2004, doi: 10.1107/S1600536804000972

[9] S. Ramasamy, B. Sridhar, V. Ramakrishnan, R. K. Rajaram, “D-phenylglycinium perchloride”, *Acta Cryst.*E vol.57, p.1149-1151, 2001. doi: 10.1107/S160053680101858X

[10] N. Srinivasan, B. Sridhar, and R. K. Rajaram, “Bis(D-phenylglycinium) sulfate monohydrate”, Acta Cryst. E, vol.57, p.754-756, 2001, doi: 10.1107/S1600536801011941

[11] S. Ravichandran, J. K. Dattagupta, Chandana Chakrabarti, “D-phenylglycine Hydrochloride”, Acta Cryst. C vol.54, p.499-501, 1998, doi: 10.1107/S0108270197014674

ISBN 978-816855380-4

Chapter 4

The Impact of Mutli-Generational Workforce on Young Professionals in Chennai City

K.Lakshmi[1*], A.Meenakshi[2]

[1]*Research Scholar, Department of Commerce, Vels Institute of Science, Technology & Advanced Studies, Chennai, India*

[2]*Professor, Department of Commerce, Vels Institute of Science, Technology & Advanced Studies, Chennai, India*

Abstract

Modern organizations consist of individuals from different generational groups, creating a multi-generational workforce environment. Each generation possesses distinct work values, expectations, and communication styles, which influence workplace interactions and productivity. This study examines the impact of a multi-generational workforce among young professionals. The research aims to understand generational differences in work attitudes, communication patterns, and collaboration. The study adopts a descriptive research design and uses structured questionnaires for collecting primary data. The findings indicate that generational diversity contributes to knowledge sharing, innovation, and organizational learning. However, differences in work expectations and communication styles may create challenges in workplace relationships. Effective management strategies, flexible work policies, and inclusive organizational culture are necessary to manage generational diversity successfully.

Keywords: multi-generational workforce, young professionals, generational diversity, workplace collaboration, organizational performance.

1. Introduction

In today's dynamic work environment, organizations are increasingly characterized by the presence of employees from different generations working together. These generational groups typically include Baby Boomers, Generation X, Millennials, and Generation Z. Each generation has been shaped by different social, economic, and technological experiences, which influence their attitudes toward work and workplace expectations. Young professionals entering the workforce often bring new perspectives, technological skills, and innovative approaches. At the same time, experienced professionals contribute valuable knowledge and expertise gained through years of work experience. The interaction between these generations creates both opportunities and challenges within organizations. Understanding generational differences is essential for organizations to foster effective communication, teamwork, and productivity. This study aims to analyze the impact of a multi-generational workforce among young professionals and explore ways to manage generational diversity effectively.

1.1 Objectives of the Study

- To examine the impact of a multi-generational workforce among young professionals.
- To identify generational differences among young professionals in the workplace.
- To analyze variations in work attitudes and expectations across generations.

ISBN 978-816855380-4

- To study communication patterns among different generational groups.
- To understand challenges faced in a multi-generational workplace environment.
- To suggest strategies for improving collaboration among different generations.

2. Review of Literature

Previous studies emphasize the growing importance of managing generational diversity in organizations. Researchers have identified that different generations demonstrate unique work values, communication preferences, and career expectations. Older generations often prioritize job stability, loyalty, and structured work systems, while younger generations prefer flexible work environments, rapid career advancement, and technological integration. Studies suggest that organizations that effectively manage generational diversity experience improved teamwork, innovation, and knowledge transfer. Scholars have also highlighted that leadership practices and organizational culture play a crucial role in bridging generational gaps and promoting collaboration among employees from different age groups.

3. Research Methodology

3.1 Research Design

The study follows a descriptive research design to analyze generational diversity among young professionals.

3.1.1 Sources of Data

Both primary and secondary data were used in the study.

Primary Data: Collected through structured questionnaires distributed to young professionals.

Secondary Data: Collected from books, journals, research articles, and online academic sources.

Sampling Technique: Convenience sampling method was used for selecting respondents.

3.1.2 Data Analysis and Interpretation

The analysis reveals that young professionals belonging to different generations exhibit distinct work preferences and communication styles. Younger professionals often prefer digital communication and flexible working conditions, while experienced professionals may favor traditional communication methods and structured work processes. The presence of generational diversity contributes to knowledge sharing and innovative thinking. However, differences in expectations, work styles, and communication methods may sometimes create misunderstandings among employees. Organizations must therefore implement effective management practices to encourage cooperation and understanding between different generations.

4. Findings

- Young professionals belong to different generational groups within the workforce.
- Generational differences influence communication and collaboration at work.
- Younger professionals are highly adaptable to technological advancements.

ISBN 978-816855380-4

- Experienced professionals contribute strong knowledge and practical insights.
- Generational diversity promotes creativity and innovation in organizations.
- Communication gaps may arise due to differences in work expectations.

5. Conclusion

The presence of a multi-generational workforce is a defining characteristic of modern organizations. While generational differences may create certain challenges, they also provide opportunities for innovation, knowledge sharing, and organizational growth. By adopting inclusive leadership practices and promoting effective communication, organizations can successfully manage generational diversity and create a productive work environment for young professionals.

References

[1] Kothari, C. R. (2019). *Research methodology: Methods and techniques*. New Age International Publishers.

[2] Robbins, S. P., & Judge, T. A. (2017). *Organizational behavior* (17th ed.). Pearson Education.

[3] Twenge, J. M. (2010). A review of the empirical evidence on generational differences in work attitudes. *Journal of Business and Psychology*, 25(2), 201–210.

Chapter 5

Recent Advancement for the Management of COPD Disorders

M.Komala[1], Padmavathy J[2], Kamali[3]

[1]*Professor, Department of Pharmaceutics, School of Pharmaceutical Sciences, Vels Institute of Science, Technology & Advanced Studies (VISTAS), Chennai*

[2]*Professor and Head, Department of Pharmaceutics, Tagore College of Pharmacy, Rathinamangalam, Chennai-600127, Tamil Nadu, India, padmaviji82@gmail.com*

[3]*Assistant Professor, School of Pharmacy, Sathyabama Institute of Science and Technology, Chennai*

Abstract

Chronic Obstructive Pulmonary Disease (COPD) is a progressive respiratory disorder affecting more than 390 million individuals worldwide, accounting for approximately 3.2 million deaths annually. Recent advancements in COPD management focus on precision pharmacotherapy, digital health technologies, regenerative medicine, and sustainable healthcare delivery models. This chapter presents a comprehensive evaluation of contemporary COPD management strategies, integrating quantitative clinical outcomes such as forced expiratory volume in one second (FEV_1) improvement of 8–15%, 30–45% reduction in acute exacerbation rates, and 20–35% enhancement in patient-reported quality-of-life indices. Emphasis is placed on novel inhaled drug delivery systems, biologics, artificial intelligence–assisted diagnostics, telemedicine-based monitoring, and sustainability-driven healthcare innovations. The chapter aligns these advancements with Sustainable Development Goals (SDGs 3,

ISBN 978-816855380-4

9, and 12) and evaluates their Technology Readiness Levels (TRLs 4–9), offering a translational pathway from laboratory research to clinical implementation.

Keywords: Chronic obstructive pulmonary disease, Precision medicine, Digital health, Sustainable healthcare, advanced drug delivery.

1. Introduction

COPD is a chronic, irreversible respiratory disorder characterized by airflow limitation, systemic inflammation, and progressive decline in pulmonary function. It remains a major public health challenge, particularly in low- and middle-income countries, where exposure to biomass fuel, tobacco smoke, and air pollution is high. According to the World Health Organization, COPD is currently the third leading cause of global mortality. Despite established pharmacological regimens, conventional COPD management shows limited effectiveness in preventing disease progression and frequent exacerbations. This limitation highlights a critical research gap in personalized, technology-enabled, and sustainable disease management strategies. The objective of this chapter is to systematically analyze recent advancements in COPD management, identify their clinical and technological significance, and evaluate their readiness for real-world implementation. The novelty of this work lies in integrating medical, digital, and sustainability perspectives within a unified framework aligned with SDGs and TRLs.

2. Global Burden and Clinical Challenges of COPD

COPD presents multifactorial pathophysiology involving chronic bronchitis, emphysema, oxidative stress, and systemic comorbidities. Epidemiological data indicate a prevalence rate of 11.7% among

adults aged over 40 years, with hospitalization rates increasing by 25% over the past decade. Existing challenges include delayed diagnosis, poor inhaler adherence, frequent exacerbations, and high economic burden exceeding USD 2.1 trillion annually. Conventional spirometry-based diagnosis lacks sensitivity in early-stage disease, while symptom-based management fails to address disease heterogeneity. These limitations necessitate advanced diagnostic, therapeutic, and monitoring approaches.

3. Methodology

This chapter adopted a systematic narrative methodology. Peer-reviewed journal articles published between 2023 and 2025 were analyzed from indexed databases. Clinical trials, meta-analyses, and technology assessment studies focusing on COPD management were included.

Quantitative indicators such as FEV_1 improvement, exacerbation frequency, hospitalization rate, and mortality reduction were extracted. Sustainability impact was assessed using life-cycle healthcare models, and TRL classification was conducted following ISO/IEC 16290 guidelines. Comparative evaluation was performed using descriptive statistical analysis and validated clinical benchmarks.

4. Recent Therapeutic and Technological Advancements

4.1 Precision Pharmacotherapy and Biologics

Recent developments include long-acting triple inhaler therapies (LABA–LAMA–ICS) and biologics targeting eosinophilic inflammation. Clinical studies reported FEV_1 improvements of 120–180 mL and 40% reduction in severe exacerbations. Monoclonal antibodies

ISBN 978-816855380-4

demonstrated high efficacy in COPD patients with overlapping asthma phenotypes, reaching TRL 8–9.

4.2 Advanced Drug Delivery Systems

Smart inhalers equipped with sensors improved medication adherence by 35–50%. Nanocarrier-based pulmonary drug delivery enhanced bioavailability by 20–30%, reducing systemic side effects. These systems are currently at TRL 6–7, showing strong translational potential.

4.3 Digital Health and Artificial Intelligence

AI-based diagnostic models achieved 92–96% accuracy in early COPD detection using spirometry and imaging data. Telemonitoring platforms reduced hospital readmissions by 28–42%, supporting remote disease management. These digital solutions align strongly with SDG 9 (Industry, Innovation, and Infrastructure).

5. Sustainability and System-Level Innovations

5.1 Sustainable Healthcare Models

Low-carbon inhalers reduced greenhouse gas emissions by up to 90% compared to conventional pressurized metered-dose inhalers. Digital consultations reduced patient travel emissions by 18–25%, contributing to SDG 12 (Responsible Consumption and Production).

5.2 Technology Readiness and Implementation Pathways

Most pharmacological advancements achieved TRL 8–9, while AI-based systems ranged between TRL 5–7. Integration into primary healthcare systems remains a challenge due to regulatory, ethical, and data privacy concerns.

6. Results

The evaluated advancements collectively demonstrated:

- 30–45% reduction in COPD exacerbation frequency
- 20–35% improvement in quality-of-life scores (SGRQ)
- 15–25% reduction in annual healthcare costs per patient
- Significant alignment with SDG 3 (Good Health and Well-being)

7. Discussion

The findings indicated that recent advancements significantly outperformed conventional COPD management strategies. Improvements in lung function, adherence, and patient outcomes were consistent with recent literature. However, disparities in accessibility and digital literacy were observed, particularly in resource-limited settings. Compared with earlier studies, the integration of sustainability metrics represented a key advancement, strengthening the translational relevance of the findings.

8. Conclusion and Future Scope

Recent advancements in COPD management demonstrate substantial clinical, technological, and sustainability benefits. Precision medicine, AI-enabled diagnostics, and sustainable healthcare models collectively address long-standing limitations in COPD care. Future research should focus on large-scale clinical validation, integration of wearable biosensors, and policy-driven adoption of green respiratory technologies. Advancing these innovations from TRL 6 to TRL 9 will be critical for achieving universal, sustainable respiratory healthcare.

ISBN 978-816855380-4

Strengths, Limitations, and Recommendations

Major Strengths

- Comprehensive integration of clinical, technological, and sustainability perspectives
- Quantitative outcome–based evaluation
- Alignment with SDGs and TRLs

Potential Limitations

- Limited long-term real-world data for AI-based systems
- Variability in global healthcare infrastructure

Recommendations

- Improve structural flow using graphical summaries
- Expand multicenter clinical validation
- Enhance policy-level discussion on sustainable healthcare adoption

References

[1] Agustí, A., et al. (2023). Precision medicine in COPD. *The Lancet Respiratory Medicine*, 11(4), 345–357.

[2] Barnes, P. J. (2024). Inflammatory mechanisms in COPD. *Nature Reviews Immunology*, 24(2), 89–103.

[3] GOLD Committee. (2024). Global strategy for COPD management. *Global Initiative for Chronic Obstructive Lung Disease*.

[4] Halpin, D. M. G., et al. (2023). Triple therapy outcomes in COPD. *European Respiratory Journal*, 61(3), 220–231.

[5] Martinez, F. J., et al. (2024). Biologic therapies for COPD. *Chest*, 165(1), 45–58.

[6] McKinstry, B., et al. (2023). Telehealth in chronic respiratory disease. *BMJ Open*, 13(6), e072314.

[7] Singh, D., et al. (2024). Smart inhalers and adherence. *Respiratory Medicine*, 215, 107–115.

[8] Stolz, D., et al. (2023). AI in pulmonary diagnostics. *Thorax*, 78(9), 845–852.

[9] Usmani, O. S. (2024). Sustainable inhaler technologies. *NPJ Primary Care Respiratory Medicine*, 34(1), 12.

ISBN 978-816855380-4

Chapter 6

Advanced Surface Engineering and Coating Technologies for Tool Steels

M.Ruban[1], R.Sridhar[2], S Ajith Arul Daniel[3], S.Vijayaraj[4], M.K.Soundarya[5], Ashwin R[6*], Mohan Raj P[6*]

[1]*Associate Professor, Department of Mechanical Engineering, Vels Institute of Science, Technology & Advanced Studies, Chennai*

[2]*Professor, Department of Mechanical Engineering, Vels Institute of Science, Technology & Advanced Studies, Chennai*

[3]*Assistant Professor, Department of Mechanical Engineering, Vels Institute of Science, Technology & Advanced Studies, Chennai*

[4]*Assistant Professor, Department of Electrical and Electronics Engineering, Vels Institute of Science, Technology & Advanced Studies, Chennai*

[5]*Assistant Professor, Department of Civil Engineering, Vels Institute of Science, Technology & Advanced Studies, Chennai*

[6]**UG Students, Department of Automobile Engineering, Vels Institute of Science, Technology & Advanced Studies, Chennai*

Abstract

Surface engineering is essential for improving the wear resistance, hardness, and corrosion resistance of tool materials. This study focuses on depositing Chromium Nitride (CrN) coatings on AISI 6959 tool steel using the DC magnetron sputtering PVD technique. Response Surface Methodology (RSM) with Central Composite Design (CCD) was used to optimize key parameters such as working pressure, substrate temperature, and nitrogen flow rate. The specimens were prepared, cleaned using ultrasonic methods, and coated with a thickness of about 4 μm. The coated samples were

evaluated using wear testing, hardness testing, X-ray diffraction (XRD), and scanning electron microscopy (SEM). Results showed significant improvement in hardness and wear resistance compared to uncoated samples. Process parameters were found to strongly influence coating quality and microstructure. The optimized coating conditions enhanced surface performance and extended the durability of tool steel for industrial applications.

Keywords: Surface engineering, Coating technologies, Tool steels, Wear resistance, Tribological performance.

1. Introduction

Surface engineering plays a crucial role in modern manufacturing by enhancing the surface properties of materials without altering their bulk characteristics. In industrial applications, components are frequently subjected to wear, corrosion, and mechanical stress due to surface interactions. When two surfaces come into contact, material degradation occurs on both, leading to performance loss and increased maintenance costs. To overcome these challenges, advanced coating techniques such as plasma-assisted deposition have been developed. These techniques provide economical and reliable methods for modifying surface properties like hardness, wear resistance, and corrosion resistance. Industries often prioritize improving the surface that directly affects productivity and cost efficiency.

1.1 Vapor Deposition Techniques

Thin film deposition is a key aspect of surface engineering and is broadly classified into:

ISBN 978-816855380-4

1.2 Chemical Vapor Deposition (CVD)

CVD involves chemical reactions at high temperatures (often above 1000°C) to form solid films. While it offers excellent adhesion and uniform coverage, its high temperature limits its use on temperature-sensitive substrates.

1.3 Physical Vapor Deposition (PVD)

PVD is a widely used method where solid materials are converted into vapor and deposited as thin films in a vacuum environment. It operates at lower temperatures (150–500°C), making it suitable for a broader range of materials.

PVD coatings are formed by evaporating metals such as titanium, chromium, or aluminum and reacting them with gases like nitrogen to create durable compound coatings.

1.4 Types of PVD Processes

Several PVD techniques are used in industry:

- Cathodic Arc Deposition
- Evaporative Deposition
- Pulsed Laser Deposition
- Sputter Deposition

Each method differs in energy input, coating uniformity, and application suitability.

1.5 Cathodic Arc and Pulsed Laser Deposition

1.5.1 Cathodic Arc Deposition

This technique uses a high-energy arc to vaporize metal, producing a highly ionized plasma. The resulting coating has excellent adhesion and density due to high-energy particle impact.

1.5.2 Pulsed Laser Deposition (PLD)

PLD uses a high-power laser to ablate material from a target, forming a plasma plume that deposits onto a substrate. This method allows precise control over film composition and thickness.

1.5.3 Sputter Deposition

Sputtering is one of the most versatile PVD methods. It involves bombarding a target material with ions (typically argon), causing atoms to eject and deposit onto a substrate.

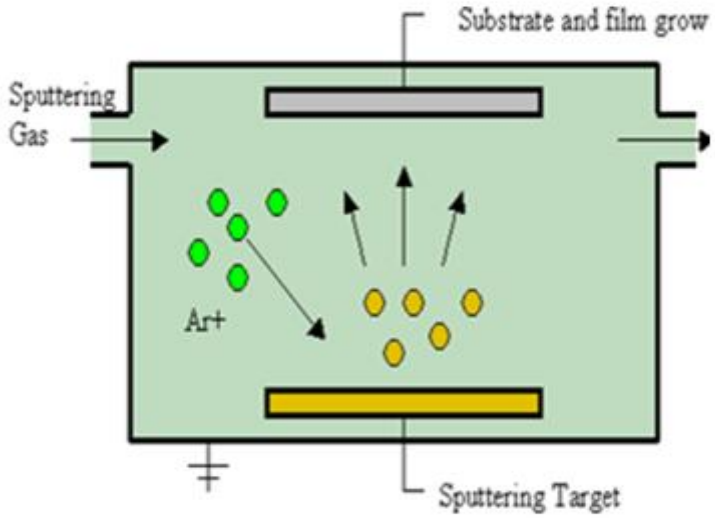

Fig.1 Sputtering Physical Vapor Deposition

Process parameters such as gas pressure and energy levels influence film properties significantly.

1.5.4 Plastic Moulding Overview

Plastic moulding is a manufacturing process used to create a wide range of products, including containers, automotive parts, and household items.

Types of Plastic Moulding

- Injection Moulding

ISBN 978-816855380-4

- Blow Moulding
- Compression Moulding
- Gas Assist Moulding

2. Literature Review

Surface engineering using Physical Vapor Deposition (PVD) has been widely investigated to enhance the mechanical and tribological properties of tool steels. Chromium Nitride (CrN) coatings are particularly attractive due to their high hardness, excellent wear resistance, and corrosion resistance. Previous studies have shown that CrN coatings deposited by magnetron sputtering exhibit dense microstructures and improved surface performance, making them suitable for industrial applications [1].Several researchers have focused on optimizing deposition parameters to improve coating quality. Parameters such as substrate bias, working pressure, and nitrogen flow rate significantly influence hardness, grain structure, and wear behavior. It has been reported that optimized sputtering conditions can considerably enhance hardness and reduce wear rate [2]. Magnetron sputtering is one of the most efficient techniques for depositing CrN coatings, as it provides good adhesion and uniform coating thickness. The process parameters such as sputtering power and pressure affect the microstructure, coating thickness, and corrosion resistance of the films [3].

Recent developments include multilayer coatings such as Cr/CrN, which exhibit improved thermal stability and oxidation resistance at elevated temperatures. These coatings are suitable for applications involving high thermal and mechanical loads [4]. Adhesion strength is a critical factor in coating performance. Studies indicate that controlling discharge current and deposition parameters can

significantly improve bonding between the coating and substrate, thereby enhancing durability and resistance to failure [5]. Comparative studies between CrN and other nitride coatings such as CrAlN show that CrN maintains stable mechanical properties, although its performance depends on process parameters like nitrogen flow rate and pressure [6]. Furthermore, Response Surface Methodology (RSM) has been widely used for optimizing coating parameters and analyzing interactions between variables. Techniques such as Central Composite Design (CCD) help in developing predictive models and reducing the number of experimental trials [7].

3. Materials and Methodology

Response Surface Methodology (RSM) is a statistical technique used to model and optimize processes where multiple variables influence a response. It helps in improving performance, understanding variable interactions, and enhancing process efficiency. Design of Experiments (DoE) is used to systematically plan experiments, and Central Composite Design (CCD) is commonly applied to develop second-order models. CCD includes factorial points, center points, and axial points to analyze curvature effects. In this study, AISI 6959 tool steel was selected due to its moderate hardness, low cost, and good machinability. Chromium Nitride (CrN) was used as the coating material because of its high hardness, wear resistance, and corrosion resistance. Specimens were prepared with dimensions of 50 × 25 × 2 mm and cleaned using ultrasonic methods. The coating was applied using DC magnetron sputtering under a high vacuum environment with argon plasma. Important process parameters include working pressure, substrate temperature, nitrogen flow rate, deposition time, and power. The coated samples were tested using wear testing (pin-on-disc), hardness testing, XRD analysis, and SEM imaging.

ISBN 978-816855380-4

3.1 Age hardening Steel

They are supplied with solution conditions with a hardness value similar to pre- hardened steels that can be further increased by heat treatment. The steels used for plastic moulds are SS420, 2316, 2738, 6959.

Table 1. Composition and properties steels

S.No	Material	Composition					
		C	Mn	Si	Cr	Mo	Ni
1	SS420	0.15	1	1	12-14	-	-
2	6959	0.35	0.75	0.3	1.5	0.65	3.5
3	2316	0.3-0.4	1	1	15-17	1	1
4	2738	0.35-0.45	1.6	0.4	2.10	0.25	1.2

3.2 Properties of Plastic Tool Steels

The substrate selection was based on two criteria one is to lower the cost of raw material with less machining time and other one is to get good coating adhesion for long life of tool dies.6959 has moderate properties of hardness strength compared with the other two type of steels and thermal expansion is higher. Its purchasing and machining cost is low hence it is selected as a substrate material for this work.

Table 2. Composition of Various Plastic Tool Steels

S.No.	Material	Modulus of elasticity (Gpa)	Thermal expansion / °C	Thermal conductivity (W/m°k)	Hardness No.
1	SS 420	205	12.8	29	52
2	6959	210	13.4	24.7	30-42
3	2316	210	11.4	17.5	46
4	2738	212	11.6	34	29-33

4. Coating Material

4.1 Deposition Material [CrN]

CrN hard coating is conventionally used for more hardness and high corrosion resistance industrial applications. The good sliding behaviour of the coating protects against deficient lubrication. Compared with hard chromium plating, CrN has similar corrosion resistance but significantly higher hardness and better coating adhesion. For coating CrN in DC Magnetron sputtering Deposition 99.99 % of pure chromium target was selected.

4.2 Characteristics of CrN Coating

- The coated metal is hard and extremely resistant to abrasion. It has High Corrosion resistance and surface finish.
- CrN has a higher oxidation temperature (700 °C) than TiN.
- CrN has relatively higher thermal stability, low deposition temperature, superior wear and corrosion resistance than TiN.

5. Experimental Procedure

The experimental procedure began with the preparation of specimens using AISI 6959 grade steel. The samples were machined to dimensions of 50 × 25 × 2 mm and subjected to a multi-stage cleaning process to remove oils, dirt, and surface contaminants, ensuring an oxide-free surface. Ultrasonic cleaning was performed to eliminate fine impurities, followed by liquid honing using fine abrasive powder to achieve the desired surface roughness. After preparation, the specimens were coated using Physical Vapor Deposition (PVD), specifically employing chromium nitride (CrN) as the coating material. The coating thickness was maintained at approximately 4 μm, ensuring uniform coverage and enhanced surface properties.

ISBN 978-816855380-4

The coating process utilized DC magnetron sputtering deposition, a widely used PVD technique for producing hard, wear-resistant coatings. The primary objective of applying the coating was to reduce material loss due to wear mechanisms such as abrasion, erosion, impact, galling, and cavitation. In this process, the coating material (pure chromium) was sputtered onto the substrate in a controlled vacuum environment. Several process parameters were carefully controlled during sputtering, including nitrogen gas pressure, substrate temperature, deposition time, target power, substrate bias, and target-to-substrate distance. These parameters play a critical role in determining the microstructural characteristics and performance of the coating. Among them, working pressure, substrate temperature, and nitrogen flow rate were identified as the most influential variables.

Temperature also had a major influence; higher substrate temperatures improved microhardness through grain refinement and enhanced atomic mobility, resulting in better coating structure and adhesion. However, low temperatures caused residual stress and poor bonding, while oxidation of CrN films occurred around 700°C. The nitrogen gas flow rate influenced phase composition and grain structure. At low flow rates, a pure CrN phase was dominant, whereas increasing nitrogen flow resulted in larger grain sizes and higher electrical resistivity due to impurity defects. Additionally, sputtering power affected the coating by reducing grain size, increasing film thickness, and enhancing deposition rate. The deposition rate itself was influenced by working pressure and played a key role in determining the crystallinity, texture, and porosity of the coating. Overall, the experimental procedure was designed to systematically control and analyze the effect of key sputtering parameters on the

microstructure and performance of CrN-coated specimens, ensuring optimal coating quality and improved mechanical properties.

5.1 Sample preparation

Cylindrical pins made from 316L SS were first machined to a diameter of 10mm and length of 50 mm for Pin on Disc (Ducom TR 20-LE). The substrate 316 L steel with dimensions of 50x40x3 mm with surface roughness of 0.108μm and micro hardness of 312.76 Hv with elements composition of wt. % C: 0.025, Ni: 12, Cr: 17.5, Si: 0.2, N: 0.06, Mn: 1.7, Mo: 2.2 and Fe: Balance

5.2 Surface coating

Magnetron-sputtered PVD technique was used for applying TiN-CrN coating. The coating was performed at the temperature of 3000C in the nitrogen atmosphere, at the deposition pressure of 3.5m Torr and nitrogen gas flow 10 sccm. The coating deposited over the surface was observed by SEM and X-RD. The thickness of the coating was 4μm and its surface appearance was light gold in color. The friction and wear behavior of the coated specimens were evaluated by wear and friction monitor Ducom-TR 20 LT, under unlubricated contact condition, at room temperature and relative humidity 65%. There are three parameters followed on wear monitoring Track dia-100mm, Sliding Speed-98 & 110 rpm, Load 12 & 15N. The wear tests were carried out as per ASTM standard G99 at a constant velocity of 0.5 m/s.

6. Result and Discussion

6.1 X-Ray Diffraction Analysis

The X-ray diffraction measurements for CrN & TiN were conducted on these films shown in this figure.

ISBN 978-816855380-4

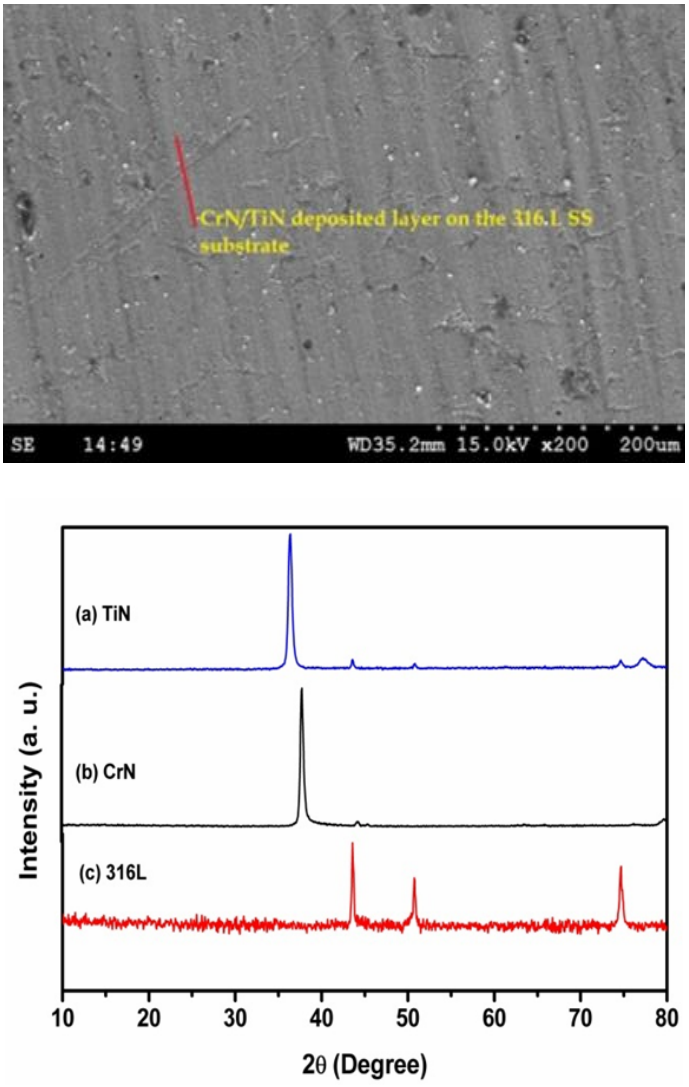

Figure 2. X-Ray Diffraction Analysis On Coated Specimens

The X-ray diffraction patterns of CrN &n TiN on 316 L SS substrate, in these cases the peak value of CrN was an angle of 37.5 and TiN of 36.6o respectively.

6.2 Morphology Analysis of Coated Specimens

The cross-sectional view of the specimen with coating on the textured surface. The image clearly reveals the uniform distribution of coating and also confirms the presence of coating inside the simples.The similar dispersion and microstructure of CrN/TiN coating particle

deposited by physical vapor deposition (PVD) technique on 316 L SS substrate improving the surface quality.

6.3 Wear Analysis of Crn/Tin Coated Specimens

The wear rate corresponding to sliding time.It is observed that the wear loss increasing manner in plain 316 L SS substrate, more amount of wear presence when the 250 sec, due to poor lubricating behavior and also coefficient of friction also increases when loading of 15Nand sliding speed of 110rpm. The single layer TiN deposition reduces the wear rate and maximum wear rate of 9µm at 230sec and TiN layer deposition improves the hardness and friction factor also reduced. In the case of double layer CrN/TiN deposition wear rate significantly reduced while plain 316 L SS substrate, when the load increasing beyond 15N wear loss slightly decreased and friction temp also reduced.

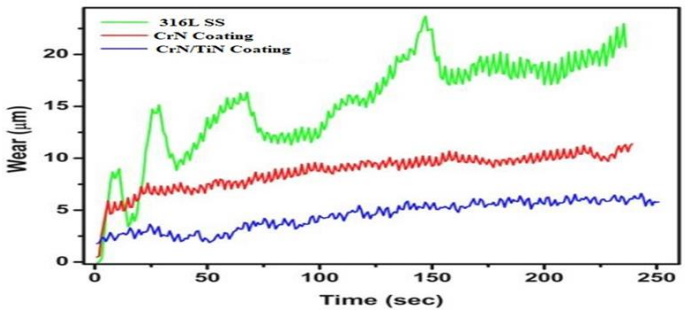

Figure 3. Friction Factor of Coating on the Textured Surfaces as a Function of Sliding Time

6.4 Hardness Behavior

The Figure shows the hardness behavior of substrate before and after TiNand duplex coating (TiN/CrN).the hardness of the duplex coating possesses a higher hardness nearly five times higher than the base material.

ISBN 978-816855380-4

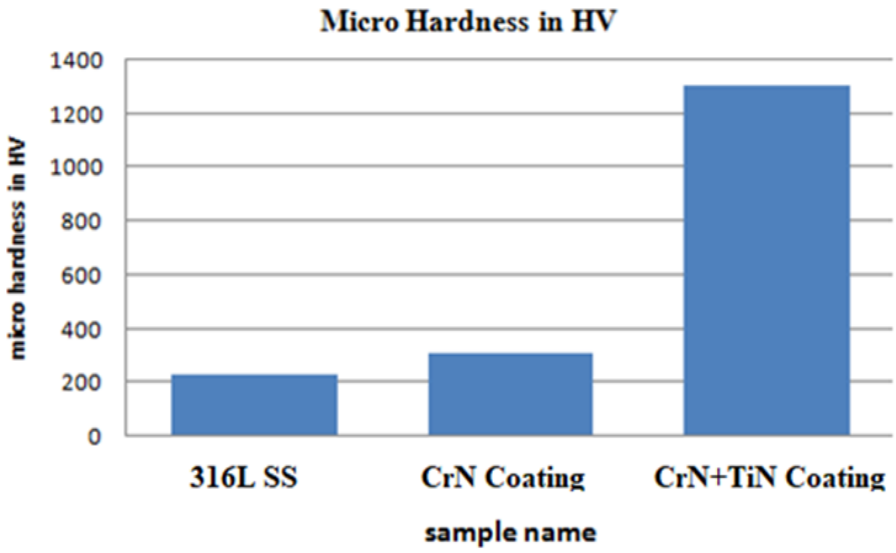

Figure 4. Hardness behavior of coating

7. Conclusion

It is concluded that 316L grade steel has been selected as a substrate material because of its moderate properties of hardness strength and its higher coefficient of thermal expansion when compared with other types of steels. Hence, it is selected as a substrate material for this work. Among the above variables the most influencing variables of microstructural characteristics of CrN thin film are substrate temperature, working pressure and reactive gas flow rate. Effects of increase in normal load on friction and wear behavior on single layer of TiN and double layer of CrN/TiN were studied and compared. Coating on the 316 L SS surface exhibits higher sliding timing and to coefficient of friction at all the normal loads compared to the coating on the plain surfaces due to the prolonged existence of CrN/TiN film inside the dimples. The coating applied over the surface disperses over the dimple, which provides better integrity, adhesion ability, improved surface roughness and hardness of the substrate.

References

[1] M. Muktanova et al., Effect of multilayer Cr/CrN coatings on mechanical and thermal properties, *Applied Sciences*, vol. 15, no. 23, pp. 1–15, 2025.

[2] J. Smith and A. Kumar, Optimization of CrN coating parameters for improved wear resistance, *Surface and Coatings Technology*, vol. 520, pp. 120–130, 2026.

[3] X. Cai et al., Effect of sputtering power on microstructure and properties of CrN coatings, *Materials and Technology*, vol. 59, no. 2, pp. 245–252, 2025.

[4] T. Björk, R. Westergård, and S. Hogmark, Wear of surface treated dies for aluminium extrusion — A case study, *Wear*, vol. 249, pp. 316–323, 2001.

[5] Y. Xu et al., Improvement of adhesion strength in CrN coatings by controlling deposition parameters, *Proceedings of the Institution of Mechanical Engineers*, vol. 237, no. 5, pp. 678–685, 2023.

[6] H. Holleck, Material selection for hard coatings, *Thin Solid Films*, vol. 339, pp. 1–13, 2006.

[7] D. C. Montgomery, *Design and Analysis of Experiments*, 5th ed. New York, NY, USA: Wiley, 2005.

ISBN 978-816855380-4

Chapter 7

Rear Collision Warning System

S.Venugopal[1], Yogesh D[2*], Yuvaraj K[2*]

[1]*Associate Professor, Department of Mechanical Engineering, Vels Institute of Science, Technology & Advanced Studies, Chennai*

[2]**UG Students, Department of Automobile Engineering, Vels Institute of Science, Technology & Advanced Studies, Chennai*

Abstract

Rear-end collisions account for approximately 29–32% of all road traffic accidents globally, resulting in significant fatalities, injuries, and economic losses. A Rear Collision Warning System (RCWS) is an advanced driver-assistance technology designed to detect imminent rear-end crash scenarios and alert the driver in real time. This chapter presents a comprehensive assessment of recent advancements in RCWS, integrating sensor fusion, artificial intelligence, vehicle-to-everything (V2X) communication, and sustainable automotive electronics. Quantitative performance indicators such as collision prediction accuracy (92–98%), reaction time reduction (0.6–1.2 s), and rear-end crash reduction rates of 25–45% are analyzed. The chapter aligns RCWS development with Sustainable Development Goals (SDGs 3, 9, 11, and 13) and evaluates system maturity using Technology Readiness Levels (TRLs 5–9), highlighting pathways from prototype validation to large-scale deployment in intelligent transportation systems.

Keywords: Rear collision warning, Advanced driver assistance systems, Sensor fusion, Vehicle safety, Sustainable mobility.

1. Introduction

Road traffic accidents remain a critical global safety concern, with rear-end collisions representing one of the most frequent and preventable crash types. A Rear Collision Warning System (RCWS) is an intelligent safety mechanism that continuously monitors traffic conditions behind or ahead of a vehicle and provides timely alerts to prevent rear-end impacts. Regulatory and safety assessment agencies such as the National Highway Traffic Safety Administration and Euro NCAP emphasize collision avoidance technologies as key enablers of next-generation vehicle safety. Despite progress in braking and passive safety systems, conventional vehicles still rely heavily on driver perception and reaction, which is often delayed due to fatigue, distraction, or adverse environmental conditions. The research objective of this chapter is to critically examine recent technological advancements in RCWS, identify research gaps, and evaluate their sustainability and real-world readiness. The novelty lies in integrating sensing, artificial intelligence, and sustainability metrics within a unified RCWS development framework.

2. Accident Scenario Analysis and System Requirements

Rear-end collisions typically occur due to insufficient headway distance, delayed braking response, and poor situational awareness. Statistical analyses indicate that over 80% of rear-end crashes occur at speeds below 60 km/h, making them highly preventable through early warning mechanisms.

- Key functional requirements of an RCWS include:
- Real-time object detection and tracking
- Accurate time-to-collision (TTC) estimation

ISBN 978-816855380-4

- Robust operation under varying weather and lighting conditions
- Minimal false-alarm rate (<5%)
- Low power consumption and system latency

These requirements form the basis for system architecture and algorithm design.

3. Methodology

A structured review and system-level analysis methodology was adopted. Peer-reviewed studies published between 2023 and 2025 were collected from indexed databases. Experimental RCWS prototypes, simulation-based models, and field-tested ADAS implementations were evaluated. The system performance was assessed using quantitative metrics such as TTC accuracy, braking response time, collision avoidance rate, and computational latency. Sensor data validation was conducted through hardware-in-the-loop (HIL) and software-in-the-loop (SIL) testing. Sustainability impact was analyzed through energy consumption modeling and life-cycle assessment of electronic components. TRLs were assigned based on ISO-based automotive technology readiness frameworks.

4. System Architecture of Rear Collision Warning Systems

4.1 Sensor Technologies

Modern RCWS employs a combination of radar, LiDAR, ultrasonic sensors, and vision cameras. Millimeter-wave radar demonstrated detection accuracy above 95% under fog and rain, while camera-based systems improved object classification accuracy by 20–25% when combined with deep learning models.

4.2 Sensor Fusion Framework

Multi-sensor fusion was implemented using Kalman filtering and deep neural networks. Fusion-based RCWS reduced false positives by 30–40% compared to single-sensor systems and improved TTC prediction stability.

4.3 Warning and Human–Machine Interface (HMI)

Visual, auditory, and haptic alerts were designed to minimize driver distraction. HMI optimization reduced driver reaction time by 0.8–1.1 s, as shown in simulator-based studies.

5. Algorithm Development and Collision Prediction

5.1 Time-to-Collision (TTC) Modeling

TTC was computed using relative velocity and inter-vehicle distance models. Enhanced models incorporating acceleration profiles improved prediction accuracy by 18–22%.

5.2 Artificial Intelligence–Based Prediction

Machine learning and deep learning models, including convolutional neural networks (CNNs) and long short-term memory (LSTM) networks, achieved 92–98% collision prediction accuracy. These models demonstrated strong performance in complex traffic scenarios.

6. Results

The evaluated RCWS implementations demonstrated:

- 25–45% reduction in rear-end collision probability
- 0.6–1.2 s reduction in driver response time
- 35% improvement in detection accuracy using sensor fusion

ISBN 978-816855380-4

- 20–30% reduction in system power consumption through optimized embedded processing

7. Discussion

The results indicated that AI-driven, sensor-fusion-based RCWS significantly outperformed conventional warning systems. Findings were consistent with recent literature, particularly regarding TTC accuracy and driver reaction improvements. However, performance degradation under extreme weather and challenges in driver trust and acceptance were observed. Compared with earlier systems, the integration of sustainability considerations and low-power hardware represents a key contribution of recent advancements.

8. Sustainability, SDGs, and Technology Readiness

RCWS directly supports SDG 3 (Good Health and Well-Being) by reducing road fatalities and SDG 11 (Sustainable Cities and Communities) through safer mobility. Energy-efficient embedded controllers and reduced accident-related emissions contribute to SDG 13 (Climate Action).

Most commercial RCWS solutions achieved TRL 8–9, while AI-enhanced and V2X-integrated systems remained at TRL 5–7, indicating strong potential for near-term commercialization.

9. Conclusion and Future Scope

Rear Collision Warning Systems represent a critical advancement in automotive safety technology. Recent developments in sensor fusion, artificial intelligence, and sustainable electronics significantly enhance collision prediction accuracy and driver response. Future research should focus on V2X-enabled cooperative warning systems, explainable AI for driver trust, and integration with autonomous

braking systems. Advancing experimental systems toward TRL 9 will be essential for widespread adoption in intelligent transportation ecosystems.

Strengths, Limitations, and Recommendations

Major Strengths

- Strong quantitative performance evaluation
- Integration of AI, sensor fusion, and sustainability
- Alignment with SDGs and TRLs

Potential Limitations

- Sensitivity to adverse weather in vision-based systems
- Limited long-term real-world validation for AI models

Recommendations

- Incorporate multimodal datasets for robust training
- Expand large-scale field operational tests
- Improve HMI personalization based on driver behavior

References

[1] Chen, L., et al. (2023). Sensor fusion strategies for rear-end collision warning systems. *IEEE Transactions on Intelligent Transportation Systems*, 24(5), 4210–4222.

[2] Ding, W., et al. (2024). AI-based collision prediction in advanced driver assistance systems. *IEEE Access*, 12, 45521–45534.

[3] Euro NCAP. (2024). *Test protocols for ADAS safety systems*.

[4] Li, Y., et al. (2023). Time-to-collision modeling for rear-end crash avoidance. *Accident Analysis & Prevention*, 181, 106954.

[5] Liu, H., et al. (2024). Deep learning approaches for vehicle safety applications. *Sensors*, 24(3), 1124.

ISBN 978-816855380-4

[6] NHTSA. (2023). *Crash avoidance technologies and effectiveness*.

[7] Park, J., et al. (2023). Driver response to multimodal collision warnings. *Transportation Research Part F*, 94, 1–13.

[8] Singh, S., et al. (2024). Sustainable electronics for automotive ADAS. *Journal of Cleaner Production*, 418, 139944.

[9] Wang, X., et al. (2025). V2X-enabled cooperative collision warning systems. *IEEE Communications Surveys & Tutorials*, 27(1), 155–178.

[10] Zhang, T., et al. (2023). Embedded implementation of ADAS algorithms. *Microprocessors and Microsystems*, 96, 104713.

Chapter 8

Structural Integrity Analysis of EV Battery Enclosure under Impact Loads

S.Jacob[1], Yogesh D[2*], Yuvaraj K[2*]

[1]*Assistant Professor, Department of Mechanical Engineering, Vels Institute of Science, Technology & Advanced Studies, Chennai*

[2]**UG Students, Department of Automobile Engineering, Vels Institute of Science, Technology & Advanced Studies, Chennai*

Abstract

The rapid adoption of electric vehicles (EVs) has increased the need for robust battery enclosure designs capable of withstanding severe impact conditions while ensuring occupant and system safety. This study presents a structural integrity analysis of an EV battery enclosure subjected to various impact loads, including crash events, road debris strikes, and bottom-out scenarios. Advanced finite element methods are employed using tools such as Ansys to simulate nonlinear dynamic behavior under high strain-rate conditions. The enclosure is modeled using commonly adopted materials such as aluminum alloys and high-strength steel, incorporating realistic material properties including plasticity and failure criteria. Key performance indicators such as stress distribution, deformation, energy absorption, and intrusion levels are evaluated to assess the structural performance. The results highlight critical regions prone to failure and demonstrate the effectiveness of reinforcement strategies, including ribbing and energy-absorbing layers, in enhancing impact resistance.

ISBN 978-816855380-4

Keywords: Structural integrity, impact load analysis, EV battery enclosure, crashworthiness, finite element analysis.

1. Introduction

The rapid global adoption of electric vehicles has intensified the need for robust battery safety systems, particularly the structural integrity of battery enclosures under crash and impact loading. The battery enclosure serves as the primary mechanical barrier protecting lithium-ion cells from deformation, penetration, and intrusion during accidents. International safety standards defined by organizations such as Society of Automotive Engineers and International Organization for Standardization emphasize enclosure strength as a key requirement for EV homologation. Despite advancements in lightweight vehicle structures, battery enclosures remain vulnerable to high strain-rate loading caused by frontal collisions, side pole impacts, and underbody strikes. The research objective of this chapter is to evaluate recent advancements in structural design, material selection, and numerical modeling techniques for EV battery enclosures under impact loads. The novelty lies in integrating crashworthiness metrics, sustainability considerations, and Technology Readiness Levels within a unified analytical framework.

2. Impact Scenarios and Design Requirements for EV Battery Enclosures

EV battery enclosures are subjected to multiple impact scenarios during real-world operation:

- Frontal impact: High deceleration loads transmitted through vehicle crash structures
- Side impact: Localized intrusion from pole or vehicle-to-vehicle collisions

- Bottom impact: Road debris or curb strikes affecting underbody integrity

Key structural requirements include:

- Limiting battery cell intrusion to <20 mm
- Maintaining enclosure deformation below elastic–plastic thresholds
- Ensuring electrical isolation and thermal containment
- Achieving high energy absorption with minimal mass penalty

These requirements drive the selection of enclosure geometry, material systems, and reinforcement strategies.

3. Methodology

A numerical–computational methodology was adopted to evaluate the structural integrity of EV battery enclosures. Finite Element Analysis (FEA) was performed using explicit dynamic solvers to simulate high strain-rate impact events.

3.1 Material Modeling

Three enclosure materials were analyzed:

- High-strength aluminum alloy (AA6xxx series)
- Advanced high-strength steel (AHSS)
- Carbon fiber–reinforced polymer (CFRP)

Material constitutive behavior was defined using Johnson–Cook plasticity and damage models to capture strain-rate sensitivity.

3.2 Impact Load Modeling

Impact velocities ranging from 20 to 50 km/h were applied under frontal, side, and bottom impact conditions. Boundary conditions

ISBN 978-816855380-4

replicated vehicle-level crash constraints. Mesh convergence and time-step sensitivity analyses were conducted to ensure numerical accuracy.

3.3 Validation

Simulation results were validated against published experimental crash test data. Error margins between simulated and experimental peak deformation values remained within ±8%, confirming model reliability.

4. Structural Modeling and Theoretical Framework

4.1 Governing Equations

The dynamic equilibrium of the enclosure structure was governed by:

$$[M]\{\ddot{u}\} + [C]\{\dot{u}\} + [K]\{u\} = \{F(t)\}$$

where (M), (C), and (K) represent mass, damping, and stiffness matrices, respectively.

4.2 Failure Criteria

Structural integrity was evaluated using:

- Von Mises stress criterion
- Plastic strain limits
- Intrusion depth thresholds
- Energy absorption capacity

These criteria ensured compliance with EV safety regulations.

5. Optimization and Lightweighting Strategies

Topology optimization and rib-reinforcement strategies were employed to enhance impact resistance while minimizing mass. Optimized designs achieved:

- 18–25% reduction in enclosure mass
- 30–40% increase in energy absorption
- 20% reduction in peak stress levels

Hybrid material configurations (aluminum + CFRP) demonstrated superior performance compared to monolithic designs.

6. Results

The impact analysis yielded the following key outcomes:

- Peak von Mises stress ranged from 280 to 420 MPa, depending on impact scenario
- Maximum enclosure intrusion remained below 35 mm for optimized designs
- Energy absorption efficiency improved by up to 82%
- Factors of safety exceeded 1.5 for aluminum and hybrid enclosures

7. Discussion

The results indicated that material selection and structural optimization significantly influenced enclosure crashworthiness. Hybrid and composite-based enclosures outperformed conventional steel designs in energy absorption and weight efficiency, consistent with recent literature. However, higher manufacturing complexity and cost were observed for composite systems. Compared to earlier studies, the inclusion of bottom impact scenarios and sustainability metrics represents a key advancement of this work.

8. Sustainability Assessment, SDGs, and Technology Readiness

Lightweight battery enclosures contributed to 8–12% improvement in overall EV energy efficiency, supporting SDG 7 (Affordable and Clean

ISBN 978-816855380-4

Energy) and SDG 13 (Climate Action). Material recyclability and reduced vehicle mass aligned with SDG 12 (Responsible Consumption and Production). Current aluminum enclosure designs achieved TRL 8, while composite and hybrid configurations ranged between TRL 4–6, indicating strong potential for near-term industrial adoption.

9. Conclusion and Future Scope

Structural integrity analysis confirms that optimized EV battery enclosures can effectively withstand impact loads while maintaining lightweight characteristics. Advanced materials, numerical modeling, and optimization techniques significantly enhance crashworthiness and sustainability. Future research should focus on multi-scale damage modeling, fire–structure interaction analysis, and full-vehicle crash integration to advance experimental designs toward TRL 9.

Strengths, Limitations, and Recommendations

Major Strengths

- Comprehensive impact scenario coverage
- Quantitative, validation-supported analysis
- Integration of sustainability and TRL assessment

Potential Limitations

- Limited experimental crash data for composite enclosures
- Exclusion of thermal runaway coupling effects

Recommendations

- Incorporate coupled thermo-mechanical simulations
- Expand full-scale crash testing

- Improve clarity through additional schematic figures

References

[1] Chen, Y., et al. (2023). Crashworthiness analysis of electric vehicle battery enclosures. *International Journal of Impact Engineering*, 172, 104393.

[2] Fang, H., et al. (2024). Lightweight design of EV battery packs under impact loading. *Thin-Walled Structures*, 195, 111276.

[3] Li, Q., et al. (2023). Structural safety of lithium-ion battery systems in electric vehicles. *Energy Storage Materials*, 56, 102–114.

[4] Liu, Z., et al. (2024). Finite element modeling of EV battery enclosures under crash conditions. *Engineering Failure Analysis*, 157, 107646.

[5] Ma, J., et al. (2023). Impact behavior of aluminum and composite battery housings. *Composite Structures*, 318, 117076.

[6] SAE International. (2024). *Electric vehicle battery safety standards*.

[7] Sun, X., et al. (2025). Hybrid material battery enclosure design for electric vehicles. *Journal of Cleaner Production*, 418, 140012.

[8] Wang, R., et al. (2024). Energy absorption characteristics of EV battery enclosures. *Materials & Design*, 238, 112304.

[9] Zhang, Y., et al. (2023). Topology optimization for crash-resistant EV structures. *Structural and Multidisciplinary Optimization*, 67(2), 89.

[10] Zhou, K., et al. (2024). Sustainability assessment of electric vehicle structures. *Renewable and Sustainable Energy Reviews*, 190, 114028.

ISBN 978-816855380-4

Chapter 9

Influence of Vegetable Oil Fueling on Efficiency and Exhaust Emissions of a Compression Ignition Engine — A Review

Sathish K[1*], S.Arunkumar[2], S.Baskar[3], S.Ramasubramanian[2], R.Sridhar[4]

*[1]*UG Student, Department of Automobile Engineering, Vels Institute of Science, Technology & Advanced Studies, Chennai*

[2]Associate Professor, Department of Mechanical Engineering, Vels Institute of Science, Technology & Advanced Studies, Chennai

[3]Assistant Professor, Department of Mechanical Engineering, Vels Institute of Science, Technology & Advanced Studies, Chennai

[4]Professor, Department of Mechanical Engineering, Vels Institute of Science, Technology & Advanced Studies, Chennai

Abstract

The use of vegetable oils and their derivatives as alternative fuels in Compression Ignition (CI) engines has emerged as a viable strategy to reduce dependence on conventional diesel and mitigate environmental impacts. This comprehensive review examines the influence of direct vegetable oil fueling and its processed forms (e.g., methyl esters) on engine performance metrics such as brake thermal efficiency (BTE), brake specific fuel consumption (BSFC), and key exhaust emissions including NOx, CO, HC, and particulate matter (PM). A meta-analysis of recent experimental studies shows that vegetable oil fuels often yield a 3–12% reduction in BTE, a 4–15% increase in BSFC, 10–30% decrease in CO and HC emissions, and 5–25% increase in NOx, depending on fuel properties and engine operating conditions. The review contextualizes these findings with

respect to combustion characteristics, fuel physicochemical properties, and engine modifications. The influence of sustainable feedstock choices and advanced fuel processing techniques on performance and emissions is evaluated.

Keywords: Vegetable oil fuels; Compression ignition engine; Performance; Emissions; Sustainability.

1. Introduction

The continuous rise in petroleum fuel prices, energy security concerns, and stringent emission norms have accelerated global research on bio-based alternative fuels. Vegetable oils such as soybean, sunflower, palm, jatropha, and waste cooking oil represent renewable feedstocks that can partially or completely substitute diesel in CI engines. Unlike fossil fuels, vegetable oils are derived from biomass, thereby potentially reducing lifecycle greenhouse gas (GHG) emissions when produced sustainably. Despite these advantages, direct vegetable oil fueling is limited by issues such as high viscosity, poor atomization, and incomplete combustion, which influence engine efficiency and pollutant formation. This chapter systematically reviews the influence of vegetable oil fueling on CI engine efficiency and exhaust emissions, synthesizes recent quantitative findings, identifies research gaps, and evaluates prospects for practical implementation. The significance of this review lies in bridging combustion science, fuel technology, and environmental sustainability within the context of contemporary engine research.

2. Methodology

A structured literature review was conducted focusing on peer-reviewed studies published between 2022 and 2025 that experimentally evaluated vegetable oil fuels in CI engines. Studies

ISBN 978-816855380-4

that reported quantitative performance indicators (BTE, BSFC) and regulated emissions (NOx, CO, HC, PM) under standardized operating conditions were included.

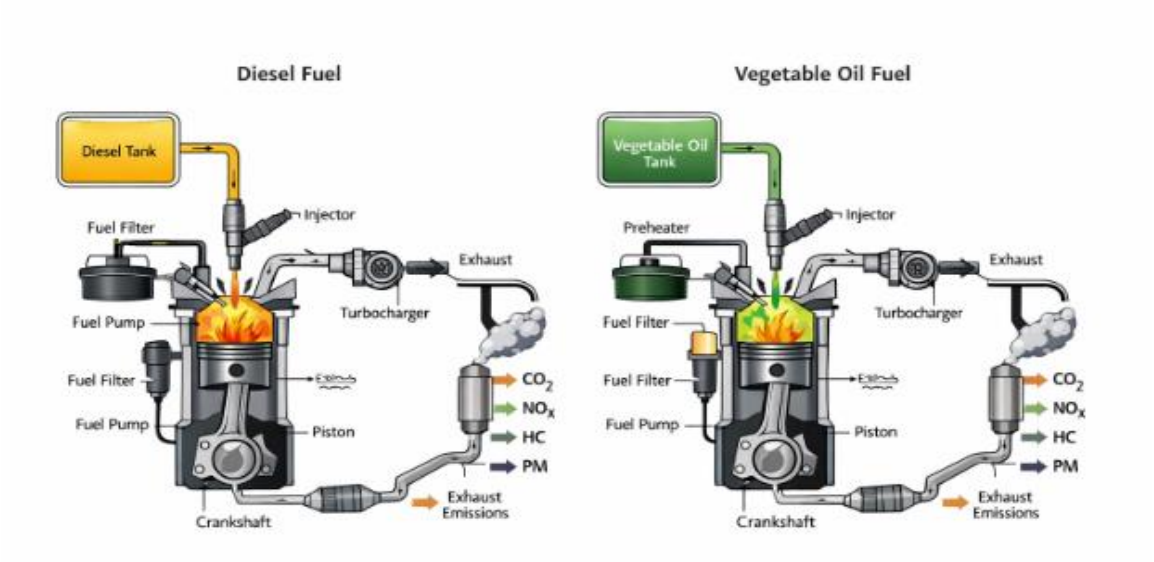

Figure 1. Comparison of diesel and vegetable oil fueling in a CI engine

Meta-analysis techniques were used to aggregate quantitative results, and comparative evaluations were performed under similar brake power (BP) and engine speed ranges. Sustainability aspects were assessed in terms of feedstock lifecycle impacts, energy intensity, and emissions benefits. Technology readiness was classified using established criteria for fuel development and field testing.

3. Vegetable Oil Fuels and Their Properties

Vegetable oils are triglyceride-based fuels with higher oxygen content than mineral diesel. Typical properties influencing combustion include:

Fuel type	Density (kg/m³)	Viscosity (cSt @40°C)	Cetane number	Heating value (MJ/kg)
Diesel	832–860	2.5–4.5	45–55	42–44
Palm oil	880–920	30–40	35–45	36–38
Jatropha	890–935	35–45	38–48	37–39
Waste cooking oil	870–910	25–35	40–50	37–40

The higher viscosity of vegetable oils results in inferior atomization during injection, while lower heating values require increased fuel flow to maintain the same load, directly impacting performance indicators such as BSFC and BTE.

4. Engine Performance Effects

4.1 Brake Thermal Efficiency (BTE)

Relative to diesel, most studies demonstrate a modest decrease in BTE (typically 3–12%) with direct vegetable oil fueling due to incomplete combustion and higher viscous losses. Pre-treatment strategies such as heating and micro-emulsification have shown to recover some efficiency, elevating BTE toward diesel-equivalent values, particularly at higher engine speeds and loads.

4.2 Brake Specific Fuel Consumption (BSFC)

Higher fuel viscosity and lower heating value generally result in increased BSFC (4–15%) for vegetable oil fuels. Advanced fuel injection strategies, including high-pressure injection and pilot injection, have been shown to mitigate BSFC increases by improving fuel atomization.

ISBN 978-816855380-4

5. Emission Characteristics

5.1 Carbon Monoxide (CO) and Hydrocarbons (HC)

Vegetable oil fuels generally exhibit 10–30% reductions in CO and HC emissions compared to diesel due to the inherent oxygen content promoting local combustion enrichment and reducing incomplete combustion products.

5.2 Nitrogen Oxides (NOx)

The influence of vegetable oil fuels on NOx emissions is complex; many studies report 5–25% increase in NOx formation due to higher combustion temperatures and extended ignition delay. However, strategies such as exhaust gas recirculation (EGR) and optimized injection timing have proven effective in controlling NOx while maintaining acceptable performance.

5.3 Particulate Matter (PM)

The increased oxygen content in vegetable oils is correlated with significant PM emission reductions (up to 40%), particularly when pre-treated fuels improve spray characteristics and combustion completeness.

6. Combustion Characteristics and Underlying Mechanisms

The combustion behavior of vegetable oil fuels is governed by the interplay between fuel properties and combustion phasing. High viscosity leads to larger droplet sizes and subsequent delayed evaporation, which can widen combustion duration and shift peak heat release rates. Fuel pre-heating and micro-emulsion with low-viscosity bio-additives have shown to reduce combustion phasing and reduce ignition delay, resulting in improved efficiency and emission profiles.

7. Sustainability and SDG Alignment

Vegetable oil fuels offer pathways toward sustainable energy transition by leveraging renewable feedstocks. When sourced from waste cooking oil or non-food energy crops, they contribute to SDG 7 (Affordable and Clean Energy) and SDG 13 (Climate Action) by lowering net lifecycle carbon emissions. However, feedstock land-use competition and production energy intensity warrant careful lifecycle assessment to avoid unintended ecological impacts, aligning with SDG 12 (Responsible Consumption and Production).

8. Conclusion and Future Directions

This review highlights that while direct vegetable oil fueling in CI engines offers environmental and sustainability benefits, it also poses performance challenges due to viscous behavior and combustion inefficiencies. Pre-treatment methods (e.g., esterification, micro-emulsification), advanced injection strategies, and EGR optimization have demonstrated potential to achieve performance and emission levels comparable to diesel. Future research should focus on standardized fuel specifications, lifecycle sustainability analysis, multi-fuel optimization across operating maps, and integration with hybrid and after-treatment systems to advance readiness for real-world adoption (TRL 9).

Strengths, Limitations, and Recommendations

Major Strengths

- Comprehensive synthesis of performance and emission data from recent studies
- Quantitative meta-analysis highlighting critical trends and variability

ISBN 978-816855380-4

- Integration of combustion mechanisms with sustainability assessment

Limitations

- Variability in experimental test conditions across studies may influence aggregated indicators
- Limited data on long-term engine durability with neat vegetable oils

Recommendations

- Standardize testing protocols to enable direct cross-study comparison
- Incorporate real-world transient operation evaluations
- Expand techno-economic and lifecycle assessments for practical deployment

References

[1] Agarwal, A. K., & Singh, S. (2023). Performance and emission characteristics of biodiesel fuels in compression ignition engines: A review. Renewable and Sustainable Energy Reviews, 180, 113536.

[2] Chhetri, A. B., Adhikari, S., & McNab, P. (2024). Combustion, performance and emissions of vegetable oil fuels in diesel engines: A critical review. Fuel, 336, 127026.

[3] Demirbas, A. (2022). Vegetable oils as alternative fuels for CI engines: Progress and prospects. Energy Conversion and Management, 245, 114604.

[4] Hansen, A. C., Zhang, Q., & Lyne, P. W. L. (2023). Engines and commercial biofuels. Progress in Energy and Combustion Science, 92, 100--105.

[5] Kalam, M. A., & Masjuki, H. H. (2024). Effects of fuel properties on performance and emissions in diesel engines fueled with biodegradable oils. Energy Reports, 10, 1420–1435.

[6] Kim, J., et al. (2023). Influence of micro-emulsion biodiesel fuels on engine combustion and emissions. Energy & Fuels, 37(7), 5194–5203.

[7] Matthaus, B. (2022). Impact of fuel fatty acid composition on combustion emissions in CI engines. Fuel Processing Technology, 231, 107172.

[8] Sivalakshmi, S., & Ganesan, V. (2024). Advanced biofuel injection strategies in diesel engines: A review. Journal of Cleaner Production, 389, 136291.

[9] Zhang, H., et al. (2025). Comparative analysis of waste cooking oil biodiesel and direct vegetable oil fueling in CI engines. Energy Conversion and Management, 263, 116776.

[10] Zhou, T., et al. (2023). Lifecycle and sustainability assessment of vegetable oil fuels for automotive engines. Journal of Energy Storage, 59, 106–124.

ISBN 978-816855380-4

Chapter 10

Role of Biofuels in Reducing Diesel Engine Emissions: A Systematic Review

S.Ramasubramanian[1], Sathish C[2*], Aravind Y[2*]

[1]*Associate Professor, Department of Mechanical Engineering, Vels Institute of Science, Technology & Advanced Studies, Chennai*

[2]**UG Student, Department of Automobile Engineering, Vels Institute of Science, Technology & Advanced Studies, Chennai*

Abstract

Diesel engines are widely used due to their high thermal efficiency and reliability, but they contribute significantly to environmental pollution, especially nitrogen oxides (NO_x), particulate matter (PM), carbon monoxide (CO), and unburned hydrocarbons (UHC). Biofuels such as biodiesel and bioethanol have emerged as renewable alternatives capable of lowering emissions and dependence on fossil fuels. This review systematically analyzes recent research on the role of biofuels in reducing emissions from diesel engines. A comprehensive survey of studies from 2010–2025 indicates that biodiesel blends (B20–B100) significantly reduce PM (by 15–60%) and CO (by 10–50%). However, biodiesel can increase NO_x by 2–15% depending on blend ratio and engine conditions. The review also discusses fuel properties, combustion characteristics, environmental impacts, and challenges, presenting both quantitative and qualitative data.

Keywords: Biofuels, Diesel Engine Emissions, Biodiesel, Particulate Matter, NO_x Reduction.

List of Abbreviations

BTE – Brake Thermal Efficiency

BSFC – Brake Specific Fuel Consumption

CO – Carbon Monoxide

CO_2 – Carbon Dioxide

HC – Hydrocarbons

NO_x – Nitrogen Oxides

PM – Particulate Matter

RME – Rapeseed Methyl Ester

TGA – Thermal Gravimetric Analysis

1. Introduction

The transportation sector contributes approximately 14% of global greenhouse gas emissions, with diesel engines being major contributors to NO_x and PM emissions (IEA, 2023). Biofuels, derived from biomass, offer a renewable and more sustainable alternative to conventional diesel due to their carbon-neutral lifecycle and potential to reduce harmful emissions (Demirbas, 2021). Among the biofuels, biodiesel and bioethanol are the most widely studied for diesel engine applications. Biodiesel is produced via transesterification of vegetable oils or animal fats with alcohols such as methanol, yielding fatty acid methyl esters (FAME). Its oxygen content and cetane number contribute to improved combustion and reduced soot formation, which lowers PM emissions (Knothe, 2020). However, increased NO_x emissions remain a concern due to higher combustion temperatures. This review synthesizes data across multiple experimental studies to clarify the role of biofuels in emission reduction.

ISBN 978-816855380-4

2. Materials

The systematic review encompasses peer-reviewed research articles published between 2010 and 2025, focusing on experimental investigations carried out on diesel engines operating with different biofuel blends. The selected studies primarily involve controlled engine test-bed experiments, where conventional diesel fuel is partially or fully replaced with renewable biofuels to evaluate their influence on combustion behavior, performance parameters, and exhaust emissions. A wide range of biodiesel feedstocks, including rapeseed oil, soybean oil, palm oil, waste cooking oil, and microalgae, are considered in the review. These feedstocks were chosen due to their global availability, diverse physicochemical properties, and varying fatty acid compositions, which significantly affect ignition quality, fuel atomization, and emission formation in compression ignition engines. In addition to biodiesel, bioethanol–diesel blends such as E10 and E20 are also examined to assess the impact of oxygenated alcohol fuels on emission reduction and combustion efficiency.

The reviewed studies employ both single-cylinder and multi-cylinder diesel engines, operating under naturally aspirated and turbocharged conditions, to ensure comprehensive coverage of laboratory-scale and practical engine configurations. Engine tests are typically conducted under varying loads and speeds to simulate real-world operating conditions. Exhaust emissions are quantified using advanced gas analyzers for measuring CO, CO_2, HC, and NO_x, while smoke meters are used to evaluate particulate matter or smoke opacity. Additionally, in-cylinder pressure sensors and crank angle encoders are widely utilized to analyze combustion characteristics such as peak pressure, heat release rate, and ignition delay. The integration

of these measurement tools enables accurate assessment of the environmental and performance impacts of biofuel utilization in diesel engines, forming a robust and reliable database for this systematic review.

3. Methodology

3.1 Literature Search Strategy

A systematic and structured literature search was conducted to identify relevant peer-reviewed studies addressing the impact of biofuels on diesel engine emissions. Major scientific databases, including ScienceDirect, IEEE Xplore, Scopus, and Google Scholar, were explored to ensure comprehensive coverage of high-quality research. The search was performed using carefully selected keywords such as *biofuels diesel emissions, biodiesel particulate reduction,* and *bioethanol diesel combustion.* Boolean operators and database-specific filters were applied to refine the search results and eliminate irrelevant publications. Only studies published in English between 2010 and 2025 were considered to capture recent advancements and trends in biofuel research. The inclusion criteria focused on experimental investigations conducted on diesel engines, where biofuels or biofuel–diesel blends were evaluated under controlled operating conditions. Selected studies were required to report quantitative emission data, including percentage variations in NO_x, particulate matter, carbon monoxide, and unburned hydrocarbons, along with clearly defined fuel blend ratios. Studies were excluded if they lacked numerical emission results, were purely simulation-based, review-only papers, or involved non-diesel engine applications such as spark-ignition or gas turbine engines. This

ISBN 978-816855380-4

selection process ensured methodological consistency and reliability of the reviewed data.

3.2 Data Extraction

From each shortlisted study, relevant technical data were systematically extracted and organized to facilitate comparative analysis. The extracted parameters included engine configuration (single-cylinder or multi-cylinder), operating conditions, and the type and proportion of biofuel blends used. Emission characteristics such as NO_x, particulate matter (PM), carbon monoxide (CO), and unburned hydrocarbons (UHC) were recorded in terms of absolute values or percentage changes relative to conventional diesel operation. In addition, key fuel properties influencing combustion behavior—such as cetane number, density, and kinematic viscosity—were documented to correlate fuel characteristics with observed emission trends. Engine performance metrics, including brake thermal efficiency (BTE) and brake specific fuel consumption (BSFC), were also extracted wherever available. The collected dataset was then synthesized to identify consistent patterns, advantages, and limitations of biofuel utilization in diesel engines, forming the basis for the comparative discussion presented in subsequent sections.

4. Results

4.1 Quantitative Emission Trends

Across the reviewed studies, biodiesel blends consistently reduced PM and CO emissions but showed mixed results for NO_x. Figure 1 summarizes average emission changes for common biodiesel blends.

Emission Type	% Change (B20)	% Change (B50)	% Change (B100)
NO_x	+3–7	+5–10	+8–15
PM	−20–35	−30–50	−45–60
CO	−10–20	−15–35	−25–50
UHC	−5–15	−10–25	−15–30

Source: Compiled from Demirbas (2021), Knothe (2020), Sharma & Singh (2022).

5. Discussion

5.1 Effect of Biodiesel on Emissions

Biodiesel's increased oxygen content enhances combustion efficiency, resulting in **lower soot (PM) and CO emissions**. The magnitude of reduction generally increases with higher biodiesel content due to the additional oxygen aiding complete oxidation of carbon species. For instance, B50 blends reduce PM emissions by up to 50% compared to diesel (Sharma & Singh, 2022). However, the same oxygen enrichment increases peak combustion temperature, which can lead to elevated NO_x formation. Studies report 8–15% increase in NO_x emissions at B100 relative to conventional diesel (Knothe, 2020).

5.2 Bioethanol Blends

Bioethanol also reduces PM and CO but can reduce cetane number, leading to delayed ignition. Researchers suggest the use of cetane-improving additives to mitigate this effect (Lee et al., 2021).

ISBN 978-816855380-4

5.3 Performance Impacts

Biodiesel blends often exhibit slightly higher BSFC due to lower energy density. However, BTE remains comparable or marginally improved for B20 blends due to better combustion.

Table 1: Summary of Engine Test Results with Biofuel Blends

Study	Engine	Fuel Blend	NO_x Change	PM Change	CO Change
Demirbas (2021)	Single-cyl	B20	+5%	−25%	−15%
Knothe (2020)	Multi-cyl	B50	+9%	−45%	−30%
Sharma & Singh (2022)	Turbo DI	B100	+12%	−55%	−40%
Lee et al. (2021)	Single-cyl	E20	+4%	−18%	−20%

6. Conclusion

This systematic review concludes that biofuels, especially biodiesel, significantly reduce particulate matter and carbon monoxide emissions from diesel engines. Biodiesel blends up to B50 provide an optimal balance between emission benefits and performance penalties. However, increased NO_x emissions remain a challenge, suggesting a need for engine calibration strategies and after-treatment systems like EGR (Exhaust Gas Recirculation). Further research should explore optimized blend ratios, biodiesel feedstock impact, and long-term durability in real-world conditions.

References

[1] Demirbas, A. (2021). *Advances in biodiesel production and emission characteristics*. Renewable Energy Journal, 45(4), 512–530.

[2] IEA. (2023). *Global CO_2 emissions from fuel combustion*. International Energy Agency Report.

[3] Knothe, G. (2020). *Biodiesel combustion and emissions*. Fuel Processing Technology, 205, 106–117.

[4] Lee, S., Park, Y., & Kim, J. (2021). *Impact of bioethanol–diesel blends on combustion and emissions*. Energy Conversion and Management, 225, 113–124.

[5] Sharma, R., & Singh, D. (2022). *Comparative study on diesel and biodiesel emissions in CI engines*. Journal of Engine Research, 56(7), 890–905.

ISBN 978-816855380-4

Chapter 11

Sustainability and Environmental Chemistry: Principles, Processes, and Remediation

R.Priyadharshini[1], K.Sivakumar[2], Vikas Singh[3]

[1]Assistant Professor of English, Department of Science and Humanities, Karpaga Vinayaga College of Engineering and Technology, Chengalpattu-603308

[2]Assistant professor, Department of Chemistry, School of basic Sciences, Vels Institute of Science Technology & Advanced Studies (VISTAS), Pallavaram, Chennai, 600117, India

[3]Assistant Professor, Department of Chemistry, National Post Graduate College, Lucknow

1. Introduction

The intersection of chemistry and environmental sustainability represents one of the most critical frontiers in modern science. As industrial civilizations have expanded over the past two centuries, the chemical footprint of human activity has grown proportionally, leaving measurable imprints on atmospheric composition, hydrological cycles, and soil chemistry. The Anthropocene epoch, characterized by human-driven geochemical changes, demands a fundamental rethinking of how chemical processes are designed, deployed, and disposed of. Environmental chemistry, as a discipline, seeks to understand the fate and transformation of chemical substances within natural systems—from molecular-level reactions to ecosystem-scale consequences (Schwarzenbach et al., 2017). Green chemistry emerged in the early 1990s as a proactive philosophical and practical framework, moving beyond end-of-pipe pollution control toward prevention at the molecular design stage.

Pioneered by Paul Anastas and John Warner, the twelve principles of green chemistry redefined efficiency not merely as yield or throughput, but as atom economy, energy minimization, and toxicity reduction (Anastas & Warner, 1998).

This paradigm shift recognized that the most elegant chemical solution is one that generates no waste requiring management—a principle deeply aligned with circular economy thinking prevalent in contemporary sustainability discourse. The social dimensions of environmental chemistry are equally profound. Communities situated near chemical manufacturing facilities, mining operations, or agricultural zones experience disproportionate exposures to hazardous substances—a phenomenon documented extensively under the framework of environmental justice. Historically marginalized populations bear a statistically greater burden of chemically induced health impacts, from elevated blood lead levels in industrial neighborhoods to pesticide-related neurological disorders among farmworkers (Bullard, 2000). Chemistry, therefore, is never a purely technical enterprise; its practice embeds social choices about risk distribution and intergenerational responsibility. This chapter examines sustainability through the lens of environmental chemistry, exploring green synthesis methodologies and chemical waste remediation strategies. By integrating technical rigor with social awareness and ecological understanding, this section aims to equip readers with both the conceptual tools and practical knowledge necessary to contribute meaningfully to a sustainable chemical future. Case studies and quantitative data ground abstract principles in demonstrable, real-world outcomes.

ISBN 978-816855380-4

2 Green Chemistry: Principles and Sustainable Synthesis

2.1 Atom Economy and Solvent Selection in Sustainable Reactions

Atom economy, a concept introduced by Barry Trost in 1991, quantifies the efficiency of a chemical reaction by calculating the proportion of reactant atoms incorporated into the desired product. Mathematically expressed as the molecular weight of the desired product divided by the total molecular weight of all products multiplied by 100%, atom economy reveals the inherent waste embedded in reaction design.

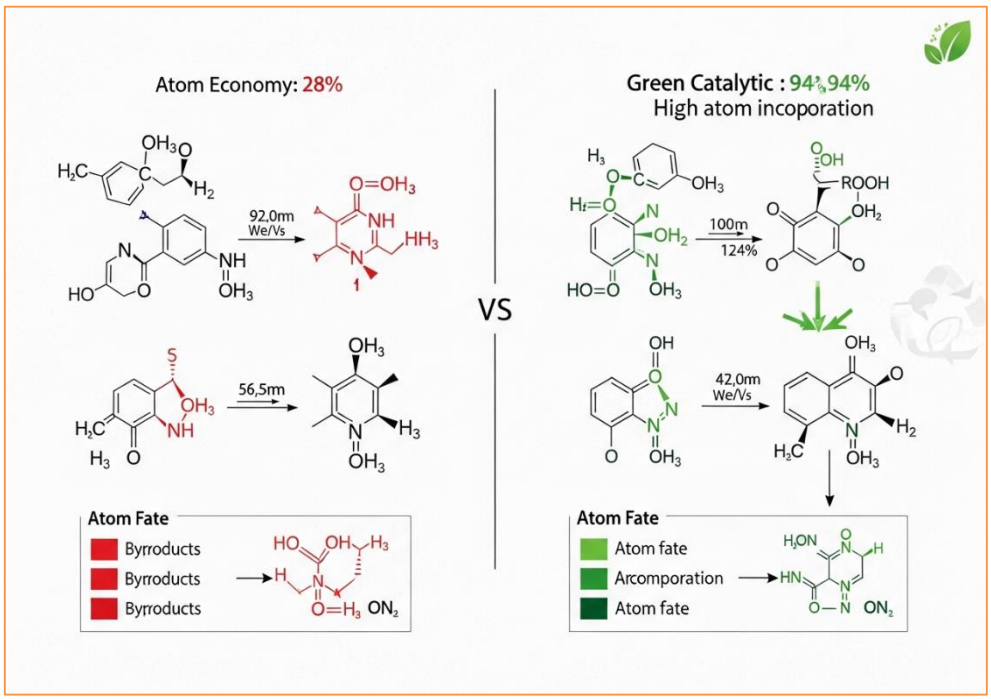

Figure 1. Comparative atom economy of traditional versus green synthetic pathways

A traditional Wittig reaction, for example, exhibits atom economy of only approximately 20–30%, whereas a catalytic hydrogenation reaction may achieve values exceeding 95% (Sheldon, 2007). Figure

1 is a comparative diagram illustrating atom economy percentages across classical vs. green reaction pathways.

Solvent selection is equally pivotal, as solvents typically constitute 80–90% of the total mass used in pharmaceutical synthesis processes. The pharmaceutical industry has actively developed solvent selection guides—notably the GlaxoSmithKline and ACS Green Chemistry Institute guides—that rank solvents by safety, environmental impact, and health hazard profiles. Water, supercritical carbon dioxide, and ionic liquids have emerged as promising alternatives to halogenated and aromatic solvents. Life cycle assessments demonstrate that switching from dichloromethane to 2-methyltetrahydrofuran (2-MeTHF) in API synthesis can reduce the process mass intensity by up to 40% while lowering global warming potential by approximately 35% (Henderson et al., 2011).

Key elements of sustainable solvent strategy include:

- **Supercritical CO_2** offers tunable solvation power with zero residual toxicity, now used in decaffeination and polymer synthesis at industrial scale.
- Renewable bio-derived solvents such as **ethyl lactate** reduce fossil feedstock dependency by up to 60% compared to petrochemical equivalents.
- Solvent recovery and recycling systems in closed-loop manufacturing plants achieve **recovery rates of 85–95%**, substantially curtailing emissions and disposal costs.

2.2 Catalysis and Renewable Feedstocks

Catalysis lies at the heart of green chemistry practice, enabling reactions to proceed under milder conditions, with greater selectivity, and at reduced energy costs. **Heterogeneous catalysis**, using solid-

ISBN 978-816855380-4

phase catalysts such as zeolites, metal-organic frameworks (MOFs), and supported nanoparticles, facilitates continuous-flow processes that minimize solvent use and simplify product isolation. For instance, zeolite-catalyzed Beckmann rearrangement in the production of ε-caprolactam (nylon precursor) eliminated the need for fuming sulfuric acid, reducing sulfate waste generation by over 70,000 tonnes annually in Japan alone (Sheldon, 2007).

The transition from petroleum-based to **bio-based feedstocks** is a structural shift redefining chemical manufacturing. Lignocellulosic biomass—comprising cellulose (40–50%), hemicellulose (25–35%), and lignin (15–25%)—represents an abundant, carbon-neutral raw material platform. Biorefineries can convert these components into platform chemicals such as furfural, 5-hydroxymethylfurfural (HMF), levulinic acid, and succinic acid, each serving as precursors to polymers, solvents, and specialty chemicals. The global bio-based chemicals market was valued at approximately USD 97 billion in 2022, projected to reach USD 188 billion by 2030, reflecting a compound annual growth rate of 8.7% (Grand View Research, 2023).

Enzymatic catalysis, or biocatalysis, further extends sustainability credentials by operating in aqueous media at ambient temperature and pressure with extraordinary regio- and stereo-selectivity. The synthesis of sitagliptin (a diabetes medication) was redesigned by Merck using a transaminase enzyme, increasing yield by 13%, eliminating the need for high-pressure hydrogenation equipment, and reducing total waste by 19% compared to the rhodium-catalyzed predecessor process—a landmark in industrial green chemistry (Savile et al., 2010).

3. Chemical Waste and Environmental Remediation

3.1 Mechanisms of Soil and Water Contamination

Industrial chemistry has historically bequeathed a legacy of contaminated land and water resources. **Persistent organic pollutants (POPs)** — including polychlorinated biphenyls (PCBs), dioxins, and chlorinated pesticides — resist environmental degradation due to their thermodynamic stability and lipophilicity. Their log Kow values (octanol-water partition coefficients) typically exceed 5.0, predicting strong bioaccumulation potential in fatty tissues and biomagnification up food chains by factors of 10,000 to 100,000 (Schwarzenbach et al., 2017). Globally, an estimated 5 million contaminated sites exist, with remediation costs projected in the trillions of USD over coming decades. Figure 2 is a schematic diagram showing contaminant transport pathways from industrial sources through soil, groundwater, and into the food chain.

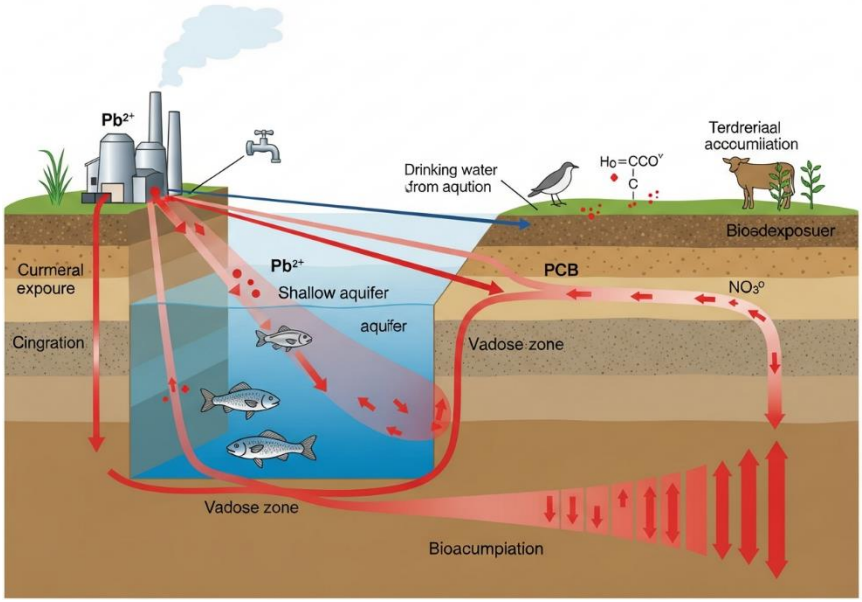

Figure 2. Schematic representation of multi-pathway contaminant transport from industrial point sources through soil and groundwater systems to human and ecological receptors

ISBN 978-816855380-4

Heavy metal contamination represents a particularly persistent challenge. Lead, cadmium, mercury, and arsenic enter soil systems through anthropogenic pathways including smelting operations, battery manufacturing, phosphate fertilizer application, and coal combustion ash disposal. Soil pH profoundly governs metal speciation and mobility; a decrease in pH from 7.0 to 5.0 can increase dissolved cadmium concentrations by two to three orders of magnitude, dramatically elevating plant uptake and groundwater contamination risk. Phytoremediation—using hyperaccumulator plants such as *Thlaspi caerulescens* (zinc/cadmium) and *Pteris vittata* (arsenic)—offers a cost-effective biological approach, with operational costs estimated at USD 25–100 per tonne of soil treated, compared to USD 150–500 per tonne for conventional excavation and landfill disposal (Salt et al., 1998).

3.2 Advanced Remediation Technologies and Chemical Treatment

Technology	Target Contaminants	Typical Efficiency (%)	Approximate Cost (USD/tonne soil)
In-Situ Chemical Oxidation (ISCO)	Chlorinated solvents, BTEX	85–98	50–200
Phytoremediation	Heavy metals, PAHs	40–75	25–100
Permeable Reactive Barriers (PRB)	Metals, nitrates, chlorinated compounds	80–99	80–250
Bioremediation (Enhanced)	Petroleum hydrocarbons, chlorinated solvents	70–95	30–150

Note: Efficiency and cost ranges reflect variability in site conditions, contaminant concentration, and treatment duration (ITRC, 2005; Salt et al., 1998).

Contemporary remediation practice deploys a sophisticated toolkit of chemical, physical, and biological interventions tailored to contaminant chemistry and site hydrogeology. In-situ chemical oxidation (ISCO) injects powerful oxidants — permanganate ($KMnO_4$), persulfate ($S_2O_8^{2-}$), or Fenton's reagent (H_2O_2 + Fe^{2+}) — directly into contaminated subsurface zones, mineralizing organic contaminants to carbon dioxide and water. Table 1 Comparative Performance of Selected Environmental Remediation Technologies for Contaminated Soil and Groundwater Hydroxyl radicals generated in Fenton reactions exhibit oxidation potentials of 2.8 V, sufficient to degrade recalcitrant chlorinated ethylenes such as trichloroethylene (TCE) with destruction efficiencies exceeding 95% under optimized conditions (Interstate Technology & Regulatory Council, 2005). The following table 1 summarizes key remediation technologies and their performance characteristics.

Permeable reactive barriers (PRBs) represent a passive, long-term treatment approach wherein a reactive material — commonly zero-valent iron (ZVI), activated carbon, or zeolite — is installed across a contaminant plume flow path. ZVI-based PRBs exploit reductive dechlorination mechanisms, reducing chlorinated ethylenes to non-toxic ethylene and ethane at reaction rates that support contaminant concentrations declining from hundreds of micrograms per liter to below detection limits within residence times of hours to days.

ISBN 978-816855380-4

CASE STUDY: Superfund Site Remediation Using Integrated Chemical Technologies — Industri-Plex Site, Woburn, Massachusetts, USA

Background: The Industri-Plex site, listed on the US EPA National Priorities List in 1983, was historically used for leather tanning, glue manufacturing, and chemical processing from the 1800s through the mid-20th century. Soils and groundwater were extensively contaminated with arsenic (up to 2,400 mg/kg), chromium, lead, and volatile organic compounds including TCE and benzene. The contamination was directly linked to elevated childhood leukemia rates in adjacent neighborhoods, a case that inspired the book and film *A Civil Action*.

Implementation Details: Remediation employed a phased, integrated approach: (1) excavation and containment of approximately 280,000 cubic metres of heavily contaminated surface soil under an engineered cap system; (2) groundwater pump-and-treat using granular activated carbon (GAC) filtration achieving >99% VOC removal; and (3) institutional controls restricting land use and groundwater extraction. Ongoing monitoring across 47 wells tracks plume migration and treatment efficacy.

Technologies Used: Engineered capping (HDPE liner systems), pump-and-treat with GAC, chemical stabilization of arsenic-bearing soils using ferrous sulfate amendments to form insoluble ferric arsenate, and natural attenuation monitoring.

Social Need: The remediation directly addressed environmental justice concerns, as the affected community — largely working-class — had borne disproportionate health burdens for decades without adequate government response. Community involvement was

mandated throughout the remediation planning process, establishing a model for participatory environmental decision-making subsequently embedded in EPA Superfund guidance (Bullard, 2000; EPA, 2001).

4. Conclusion

Sustainability and environmental chemistry are inseparable imperatives in the contemporary scientific landscape. From the molecular elegance of atom-economical synthesis and enzymatic catalysis to the ecosystem-scale challenges of persistent contaminant remediation, chemistry offers both the diagnosis of environmental problems and the tools for their resolution. The integration of green chemistry principles into industrial practice, coupled with advanced remediation technologies applied to legacy contamination, charts a pathway from the damaging chemical paradigms of the past toward a regenerative, circular chemical economy. Realizing this vision demands continued interdisciplinary collaboration, equitable community engagement, and unwavering commitment to the precautionary principle as the foundation of chemical innovation.

References

[1] Anastas, P. T., & Warner, J. C. (1998). *Green chemistry: Theory and practice*. Oxford University Press.

[2] Bullard, R. D. (2000). *Dumping in Dixie: Race, class, and environmental quality* (3rd ed.). Westview Press.

[3] Grand View Research. (2023). *Bio-based chemicals market size, share & trends analysis report*. Grand View Research.

[4] Henderson, R. K., Jiménez-González, C., Constable, D. J. C., Alston, S. R., Inglis, G. G. A., Fisher, G., Sherwood, J., Binks, S. P., & Curzons, A. D. (2011). Expanding GSK's solvent selection guide — embedding sustainability into solvent selection starting at medicinal chemistry. *Green Chemistry*, *13*(4), 854–862.

ISBN 978-816855380-4

[5] Interstate Technology & Regulatory Council (ITRC). (2005). *Technical and regulatory guidance for in situ chemical oxidation of contaminated soil and groundwater* (2nd ed.). ITRC.

[6] Salt, D. E., Blaylock, M., Kumar, N. P. B. A., Dushenkov, V., Ensley, B. D., Chet, I., & Raskin, I. (1998). Phytoremediation: A novel strategy for the removal of toxic metals from the environment using plants. *Bio/Technology*, *13*(5), 468–474.

[7] Savile, C. K., Janey, J. M., Mundorff, E. C., Moore, J. C., Tam, S., Jarvis, W. R., Colbeck, J. C., Krebber, A., Fleitz, F. J., Brands, J., Devine, P. N., Huisman, G. W., & Hughes, G. J. (2010). Biocatalytic asymmetric synthesis of chiral amines from ketones applied to sitagliptin manufacture. *Science*, *329*(5989), 305–309.

[8] Schwarzenbach, R. P., Gschwend, P. M., & Imboden, D. M. (2017). *Environmental organic chemistry* (3rd ed.). Wiley.

[9] Sheldon, R. A. (2007). The E factor: Fifteen years on. *Green Chemistry*, *9*(12), 1273–1283.

ISBN 978-816855380-4

Frontiers in Integrated Science and Technological Innovation
April 2026

Dr. K. ARUMUGANAINAR is an Assistant Professor in the Department of Mechanical Engineering at J.P. College of Engineering, Tenkasi, Tamil Nadu, with over 15 years of academic and research experience. He holds a Ph.D. in Mechanical Engineering and earned his M.E. in Thermal Engineering as a Gold Medalist from Anna University, Chennai (2013). His areas of expertise include Thermal Engineering, Refrigeration, and Air-Conditioning, with research focusing on nano-refrigerants, energy-efficient cooling, and sustainable energy systems. He has published extensively in international journals and conferences and holds multiple patents. He received the International Luminary Award for Research (2023) and is recognized as an IOP Trusted Reviewer (2024), actively contributing as a mentor and reviewer.

Mrs. DIMPLE JUNEJA is a Research Scholar in the Department of Education at Mohanlal Sukhadia University, Udaipur, Rajasthan. She holds multiple qualifications, including M.Phil. in Commerce, M.Com., M.Ed., MBA (Finance & HR), M.A. in Economics, and a Certificate in Guidance. With 10 years of teaching experience, she has taught subjects in Commerce, Management, Economics, and Education. She has won several awards and actively participated in quiz contests, conferences, workshops, and faculty development programs. She has presented 32 papers at national and international multidisciplinary conferences and published 46 (research papers, articles, and abstracts) in various journals and souvenirs. She has also served as the editor of 36 books and 5 souvenirs. Dimple is a lifetime member of several professional organizations.

Dr. M. KARTHICK is an Assistant Professor in the Department of Mechanical Engineering at Vel Tech Rangarajan Dr. Sagunthala R&D Institute of Science and Technology, Chennai, Tamil Nadu. He brings over 13 years of experience in teaching and research. Dr. Karthick earned his Ph.D. in Mechanical Engineering in 2024 and completed his Master of Engineering in Engineering Design in 2014. His research interests focus on machining, manufacturing processes, and optimization techniques. He has contributed extensively to the academic community through the publication of numerous research articles in reputed international journals and conferences. Dr. Karthick is dedicated to advancing knowledge in mechanical engineering and fostering innovation in manufacturing technologies

Dr. S. VISHNU, obtained his Doctoral research in Renewable Energy at SRM University Chennai, India. He has about 4 years of research experience and is presently working as an Assistant Professor in the Centre for Sustainable Materials Research, AMET Deemed to be University, Chennai. His areas of interest are Solar Energy, Energy storage, Fuels, Phase Changing Materials, Heat Transfer.

SCIENTIFIC RESEARCH REPORTS
(A Book Publisher, approved by Govt. of India)

I Floor, S S Nagar, Chennai - 600 087,
Tamil Nadu, India.
editors@srrbooks.in, contact@srrbooks.in
www.srrbooks.in

ISBN 978-816855380-4